

THE FERMI-PASTA-ULAM PROBLEM: PARADOX TURNS DISCOVERY

Joseph FORD

School of Physics, Georgia Institute of Technology, Atlanta, GA 30332, USA



NORTH-HOLLAND

THE FERMI–PASTA–ULAM PROBLEM: PARADOX TURNS DISCOVERY*

Joseph FORD

School of Physics, Georgia Institute of Technology, Atlanta, GA 30332, USA

Editor: D.K. Campbell

Received August 1991

Contents:

1. Introduction	273	5. The ding-a-ling model	300
2. Background	276	6. Discussion	304
3. Integrable approximations	281	Appendix A. Algorithmic complexity theory	306
4. The transition to chaos	286	References	309

Abstract:

This pedagogical review is written as a personal retrospective which seeks to place the celebrated Fermi, Pasta, and Ulam paradox into historical perspective. After stating the Fermi–Pasta–Ulam results, we treat the questions it raises as a pedagogical “skeleton” upon which to drape (and motivate) the evolving story of nonlinear dynamics/chaos. This review is thus but another retelling of that story by one intimately involved in its unfolding. This is done without apology for two reasons. First, if my colleagues have taught me anything, it is that an audience of experts will seldom pay greater attention than when, with some modicum of grace and polish, they are told things they know perfectly well already. Second, if generations of students have taught me anything, it is that few things fascinate them more than a scientific mystery – and the Fermi–Pasta–Ulam paradox is a cracker-jack mystery. And so readers, especially graduate students curious about nonlinear dynamics/chaos, are now invited to sit back, loosen their belts (and minds), and prepare for fact that sometimes reads like fantasy.

* This work was supported in part by National Science Foundation Grant PHY-9015496.

1. Introduction

In the early 1950s MANIAC-I had just been completed and sat poised for an attack on significant problems. On one of his several visits to the Los Alamos Scientific Laboratory during this period, Enrico Fermi joined mathematician Stan Ulam and computer scientist John Pasta in a quest for suitable problems. They each recognized that MANIAC-I could answer questions holding great interest for mathematics and physics, but which one deserved immediate attention? After reflecting on the matter, Fermi suggested that it would be highly instructive to integrate the equations of motion numerically for a judiciously chosen, one-dimensional, harmonic chain of mass points weakly perturbed by nonlinear forces. Specifically, he pointed out that the shape of such a chain could not be predicted accurately by anyone after the elapse of a few hundred or so harmonic periods. Eventually, Fermi–Pasta–Ulam (FPU) intended to use this model to answer various sophisticated questions related to irreversible statistical mechanics, but the initial studies were intended merely to test the simplest and most widely believed assertions of equilibrium statistical mechanics such as equipartition of energy, ergodicity, and the like.

After much back and forth, FPU decided to numerically integrate the weakly nonlinear, fixed-end, one-dimensional chain of $(N - 1)$ moving mass points having the Hamiltonian

$$H = \sum_{k=1}^{N-1} \frac{1}{2} P_k^2 + \frac{1}{2} \sum_{k=0}^{N-1} (Q_{k+1} - Q_k)^2 + \frac{\alpha}{3} \sum_{k=0}^{N-1} (Q_{k+1} - Q_k)^3, \quad (1)$$

where $Q_0 \equiv Q_N \equiv 0$ and Q_k and P_k are the coordinate and momentum for the k th particle, where α is a small nonlinear coupling parameter, and where the particle mass M and harmonic spring constant K have been eliminated by a standard canonical transformation and a change of time scale. Concurrently, FPU also considered chains of particles whose Hamiltonians had quartic or broken linear couplings as well as the cubic nonlinearity explicitly written above. But first, like all good senior scientists sporting a brand new idea, FPU began looking for someone to do the actual work. Here they were extremely fortunate to find Mary Tsingou, who programmed the dynamics, ensured its accuracy, and provided graphs of the results. Numerical integration was carried out in terms of the particle coordinates which appear in eq. (1). But because the weak nonlinear terms in the FPU oscillator systems primarily serve only to cause energy sharing between the unperturbed harmonic normal modes, it becomes natural to present the final results in terms of normal mode coordinates A_l specified by

$$A_l = \sqrt{(2/N)} \sum_{k=1}^{N-1} Q_k \sin(kl\pi/N).$$

In terms of these coordinates, Hamiltonian (1) breaks into a sum of independent harmonic oscillators weakly coupled by terms cubic in the normal mode position variables as revealed by the following Hamiltonian:

$$H = \frac{1}{2} \sum (\dot{A}_k^2 + \omega_k^2 A_k^2) + \alpha \sum C_{klm} A_k A_l A_m, \quad (2)$$

where $\omega_k = 2 \sin(k\pi/2N)$ is the frequency of the k th normal mode, where explicit expressions for the

constants C_{klm} are not needed here, where the dot over A_k denotes time derivative, and where $E_k [= \frac{1}{2}(\dot{A}_k^2 + \omega_k^2 A_k^2)]$ is defined to be the energy in the k th normal mode. Finally, because the FPU nonlinear terms are almost always small relative to the harmonic terms, we note that $H \approx \sum E_k$ to a good approximation.

And now at last the stage is set. As FPU await the initial results from Mary Tsingou, they do so without the slightest a priori hint they have tacitly met a significant criterion enunciated some years later by the noted Soviet mathematician Dima Arnol'd: "The only computer experiments worth doing are those that yield a surprise!" Mary Tsingou now enters (stage left) bearing the *surprise* (see fig. 1). At time $t = 0$ in fig. 1, an $N = 32$, fixed-end chain governed by Hamiltonian (1) with $\alpha = 1/4$ was started at rest in the shape of a half sine wave given by $Q_k = \sin(k\pi/32)$ and then released; in other words, only the fundamental harmonic mode was initially excited and given amplitude $A_1 = 4$ and energy $E_1 = 0.077 \dots$. During the time interval $0 \leq t \leq 16$ in fig. 1, where t is measured in periods of the fundamental mode, modes 2, 3, 4, etc., sequentially begin to absorb energy from the initially dominant first mode as one would expect from an infinitesimal analysis due to Rayleigh. Following this, the pattern of energy sharing undergoes a dramatic change. Energy is now exchanged primarily only among modes 1 through 6 with all higher modes writhing about in the noise gasping for energy. Incredibly enough, the energy sharing pattern revealed in fig. 1 for this few-body anharmonic system is remarkably similar to that observed in the laboratory for few-body harmonic systems. Indeed, the motion of this nonlinear system appears to be not only almost-periodic but perhaps even quasi-periodic. The first major near-period (FPU recurrence) of the motion occurs at about $t \approx 157$ fundamental periods. Here, the energy in the fundamental mode returns to within 3% of its value at $t = 0$! FPU immediately recognized that these results were simply astounding. First, they appear to violate the canons of

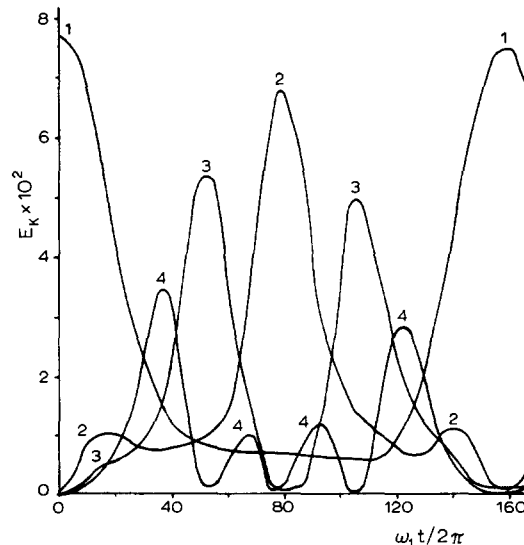


Fig. 1. A plot of the normal mode energies $E_k = \frac{1}{2}(\dot{A}_k^2 + \omega_k^2 A_k^2)$ for $N = 32$ and $\alpha = 1/4$ in Hamiltonian (2). The energy in the cubic nonlinear terms of Hamiltonian (2) never exceeded about 10% of the total energy. Mode 1 was initially given all the energy with the expectation that in time all modes would share the energy equally among themselves. But in fact, modes 6 through 32 were forever left lying in the "noise" gasping for energy. Equally surprising is the short-term recurrence indicating that the motion is almost-periodic, perhaps even quasi-periodic.

statistical mechanics, which assert that this nonlinear system should exhibit an approach to equilibrium with energy being shared equally among all degrees of freedom. But even more astonishing, they seem to invalidate Fermi's theorem regarding ergodicity in nonlinear systems. Indeed, Fermi is said to have remarked that these results might be one of the most significant discoveries of his career.

A preprint [1] describing these results was completed in May of 1955 and given limited distribution in November of that year. Then catastrophe struck; Fermi died of cancer! Temporarily, the question of what to do about the preprint faded into the background and remained there for some time. When the matter was eventually taken up, Pasta and Ulam found themselves trapped: they clearly could not publish *without* Fermi's name on the paper, but equally they could not publish *with* Fermi's name on the paper, since he had neither read nor approved it. This dilemma was never resolved, and, as a consequence, the FPU results were never published. However, the manuscript did finally reach the open literature as part of Fermi's collected works [2], which appeared some ten years after distribution of the original FPU preprint.

One can only speculate about the impact immediate publication of this work might have had. Although the FPU preprint received fairly wide circulation in the statistical mechanics community, it was after all only a preprint. Perhaps because it did not bear the seal of reviewers' and editors' approval nor carry the authority of a living Fermi, many readers of the preprint felt freer than usual to accept their own handwaving conjectures as proper explanation of the FPU paradox. Some thought that FPU had merely failed to integrate Hamiltonian (1) long enough. They suggested that the thermalization process simply took longer than anticipated. Here, it was thought that the 3% lack of closure upon first return seen in fig. 1 might widen to 6% or greater on the second return, and grow to 9% or greater on the third, etc. Others believed that the weak, broken linear or polynomial nonlinear forces used by FPU were much too simple to accurately describe physical reality. Still others remarked that, since one-dimensional systems were commonly assumed to be incapable of exhibiting a normal thermal conductivity, such systems were especially unlikely candidates for exhibiting a proper approach to equilibrium. Some few even suggested that the FPU recurrence was merely a Poincaré recurrence. All these arguments have two things in common. They resolve the FPU paradox by trivializing it, and they offer resolutions unsupported by the slightest shred of hard evidence. Of course, the vast majority of readers were simply puzzled by the FPU manuscript and had no explanation to offer. Regardless, everyone found the preprint to be quite startling and equally fascinating; however, almost no one recognized it as a harbinger of a new era in physics. But, in fact, the FPU calculations exposed a genuine paradox whose unfolding resolution has unleashed winds of change destined to blow far, far into the 21st century. In this personal retrospective, we shall gauge these winds and seek to place the work of Fermi, Pasta, and Ulam in proper historical perspective.

Specifically, section 2 presents the background material needed to recognize that the FPU results do represent a genuine paradox. Section 3 then discusses the early attempts to resolve the paradox via integrable approximations. Section 4 at last reveals the chaotic behavior lurking just beneath the FPU calculations by linking FPU to the classic Hénon–Heiles system. Section 5 then achieves FPU's original aim of demonstrating the appearance of a normal thermal conductivity and an approach to equilibrium in a simple mechanical model. Concluding remarks are presented in the final section 6. Finally, let us emphasize here at the outset that, while this article seeks not only to resolve the FPU paradox but to use it as a pedagogical device for surveying, at the graduate student level, much of nonlinear dynamics/chaos, our review is not intended to be encyclopedic. The choice of topics as well as the emphasis assigned to them is based solely on the personal taste of the present author.

2. Background

FPU expected the motion of their coupled oscillator systems to be stochastic^{*)} whereas their computer calculations revealed the motion to be highly ordered, perhaps analytically solvable. But should we not be startled that researchers as sophisticated as FPU could make such a misjudgment some three hundred years after Newton? For, given the FPU Hamiltonian, does not dynamics provide an easily applied test predicting the character of the motion which ensues? In FPU's defense, let us quickly admit that there is no such test, only folklore supported by prejudice. Classical mechanics frequently claim that the few-body problem is analytically solvable, hence nonstochastic, but they noticeably omit defining how many is "few". Taking the opposite tack, statistical mechanics assert that the many-body problem is stochastic, but they noticeably omit giving a proof. Moreover, this folklore runs afoul of well-established fact. Poincaré [3] recognized decades ago that the gravitational three-body problem is stochastic; equally, classical perturbation [4] theory has no difficulty exhibiting many-body systems which can easily be solved analytically. But let us now add additional spice to this narrative by remarking that in his youth Fermi published a theorem [5] (a synopsis of the theorem appears in ref. [6, p. 358]) which proves that the FPU system is stochastic! In order to proceed further, we must now develop the background which will permit us to unravel this tangle of confusions.

To begin, recall that any Hamiltonian system with N degrees of freedom always has $2N$ constants of the motion but only $(2N - 1)$ of them can be time independent [6]. Let us verify these facts. The solution to Hamilton's equations reads $Q_k = Q_k(Q_{l0}, P_{l0}, t)$, $P_k = P_k(Q_{l0}, P_{l0}, t)$, where the Q 's are position variables and the P 's are momentum variables and where k and l run from 1 to N . Now solve any one of these $2N$ equations for the time t and substitute the resulting expression for t in each of the remaining $(2N - 1)$ equations. These $(2N - 1)$ time-independent equations relating initial to final (Q_k, P_k) define the time-independent constants of the motion. The remaining equation which was solved for the time can be brought to the form $F(Q_{k0}, P_{k0}, Q_k, P_k, t) = 0$. F is thus seen to be a constant of the motion despite its explicit dependence on time. Geometrically, the common intersection of the $(2N - 1)$ time-independent constant of the motion surfaces in phase space defines a system orbit. The time-dependent constant F determines the starting point on the orbit.

Such a plethora of constants of the motion for Hamiltonian systems would, at first blush, seem to imply that all Hamiltonian motion is highly ordered, nonstochastic, and perhaps even analytically integrable. Indeed, well into this century many investigators held the belief that Newtonian systems should be viewed not as nonintegrable but rather as not yet integrated. Alas, we now know that such is not the case, for in general most of the $(2N - 1)$ constants are multivalued, pathological monstrosities which permit orbits to wander as freely over the energy surface $H = E$ as if they did not exist.

This then suggests that by restricting our attention to Hamiltonian systems having well-behaved constants of the motion, we might obtain a class of systems which is nonstochastic and solvable. Indeed, *integrable systems* [7] are precisely of this desired type. An integrable Hamiltonian system is defined as one having as many single-valued, analytic (in the sense of complex variable theory) constants of the motion Φ_k as degrees of freedom such that all pairwise Poisson brackets $[\Phi_k, \Phi_l] = 0$. However, the true meaning of integrability is exposed in the following definition [8]. A Hamiltonian $H(q_k, p_k)$ is said to be integrable if there exists a single-valued, analytic, canonical transformation bringing $H(q_k, p_k)$ to

^{*)} Stochastic is a term frequently, but not exclusively, used in the Soviet literature to mean deterministic motion which, without any externally imposed randomness, has some of the properties of a stochastic process. In the contemporary literature, "stochastic" has been replaced by "chaos", which is discussed at length in appendix A.

the form $\mathcal{H}(\mathcal{P}_k)$, i.e., a function of the new momenta \mathcal{P}_k alone. Each new momentum \mathcal{P}_k is clearly a constant of the motion; moreover, the Poisson brackets $[\mathcal{P}_k, \mathcal{P}_l] = 0$ for all \mathcal{P}_k – \mathcal{P}_l pairs, in agreement with our earlier definition. But now comes the moment of truth. In the new coordinates, Hamiltonian’s equations are seen to be integrable precisely because they have been brought to a form which is trivial to integrate. Specifically, $\dot{\mathcal{P}}_k = 0$ and $\dot{\mathcal{Q}}_k = Q_k(\mathcal{P}_l)$ have the obvious solutions $\mathcal{P}_k = \mathcal{P}_{k0}$ and $\mathcal{Q}_k = \omega_k t + Q_{k0}$, where $\omega_k \equiv \partial \mathcal{H} / \partial \mathcal{P}_k$.

For integrable Hamiltonian systems whose motion is spatially bounded – the only type we shall consider in this paper – the \mathcal{Q}_k are angles and the ω_k are therefore angular frequencies. In transformed coordinates, the motion for an integrable system is easily visualized [9] since it is topologically equivalent to motion on a torus – see fig. 2. Here for the case of two degrees of freedom, the momentum variables \mathcal{P}_k and the position variables \mathcal{Q}_k may be regarded as labels for the actual “radii” and angular positions on the two-dimensional toroidal surface. At fixed energy $\mathcal{H} = E$, the momenta \mathcal{P}_1 and \mathcal{P}_2 are not independent, leading to the toroidal nesting [10] shown in fig. 2. When the system has $N \geq 3$ degrees of freedom, system motion occurs on surfaces of N -tori, difficult to visualize or draw, but still conceptually simple. The only unusual feature is that for $N = 2$, each 2D toroidal surface divides the 3D energy surface into an inside and an outside; however, for $N \geq 3$, the toroidal surfaces of N dimensions can no longer divide energy surfaces having $(2N - 1)$ dimensions. Only a bit of thought is

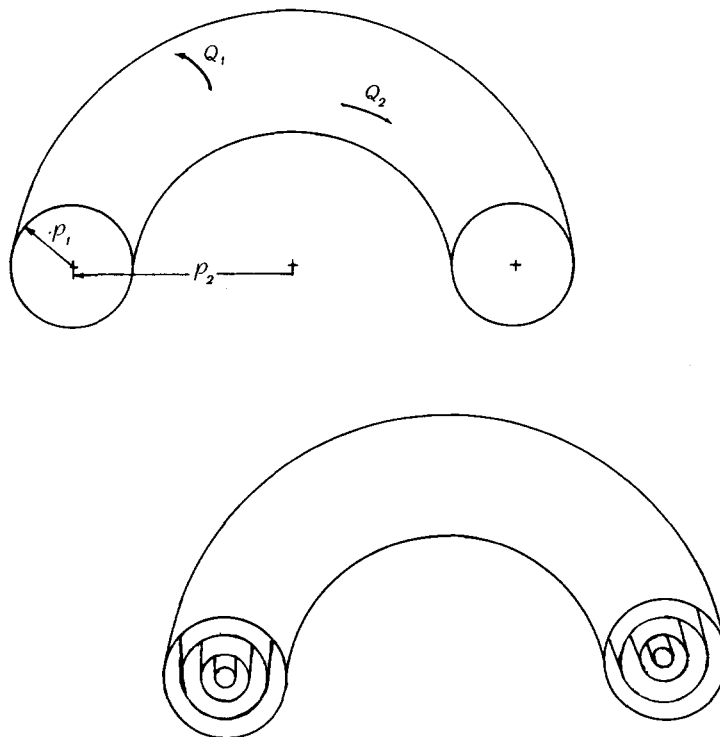


Fig. 2. Topologically speaking, the orbits of integrable systems may be regarded as lying on the surfaces of tori, where the momenta and angle coordinates may be viewed as labels for radii and angles on the toroidal surfaces. Specifically, a typical torus for a two degrees of freedom system is shown at the upper left, where momenta and angles have been written in, but one must bear in mind that, on this topological drawing, the \mathcal{P}_k and \mathcal{Q}_k are only labels. In the lower figure, we observe that, since the two momenta are not independent due to conservation of energy, the energy surface is striated by nested tori as shown.

needed to verify this seemingly trivial fact, which gains in significance when one notes that it leads to Arnol'd diffusion [11, 12] a topic to which we shall return later.

In transformed coordinates $(\mathcal{Q}_k, \mathcal{P}_k)$, integrable system motion is quasi-periodic with as many basic frequencies ω_k as degrees of freedom. Because the inverse canonical transformation carrying us from new coordinates $(\mathcal{Q}_k, \mathcal{P}_k)$ back to original coordinates (q_k, p_k) is in general nonlinear, not only the basic frequencies ω_k but all sum and difference frequencies $(m\omega_k \pm n\omega_l)$ may also appear in the motion. To the naked eye, integrable motion involving such a multitude of frequencies can for a time look like random noise, but then near-periodicities and the structure of its frequency spectrum reveal its underlying simplicity. With these points in mind, it is tempting to suggest that the FPU motion revealed in fig. 1 is integrable. There are several reasons why this conclusion would be premature, and we now proceed to discuss one of them.

Let us now consider the class of analytic Hamiltonians having an equilibrium point (FPU, for example), that is, Hamiltonians $H(Q_k, P_k)$ which can be expanded in convergent power series about their equilibrium points. We may then require that the leading quadratic terms have the form $\frac{1}{2} \Sigma (P_k^2 + \omega_k^2 Q_k^2)$, again like FPU. It then follows that each such Hamiltonian is one to one with its unique set $\{C_k\}$ of power series expansion coefficients, where the subscript symbol k denotes a $2N$ -dimensional vector subscript having integer components and where N is the number of system degrees of freedom. We are now at liberty to regard each Hamiltonian $H(Q_k, P_k)$ as a point in an infinite dimensional, Euclidean space in which the k th mutually perpendicular axis bears the coordinate C_k . This prologue then permits us to state the following deep theorem due to Siegel [11].

Theorem. In every neighborhood of such an analytic Hamiltonian, whether integrable or not, there exists a nonintegrable Hamiltonian.

This theorem provides our first glimpse of the fact that nonintegrable systems are “thick as fleas” in C_k -space while integrable ones are, relatively speaking, “scarce as hen’s teeth”. Specifically, it tells us that, if we slightly change the expansion coefficients of an integrable Hamiltonian, we in general obtain a nonintegrable one whereas slight changes in a nonintegrable system simply shift it into another nonintegrable system.

An intuitive understanding of this theorem may be gained from an examination of the phase plane (ρ, ϕ) portrait for an integrable pendulum as shown in fig. 3. Here the closed ovals represent simple oscillations; the top and bottom curves in the figure represent motion in which the pendulum goes

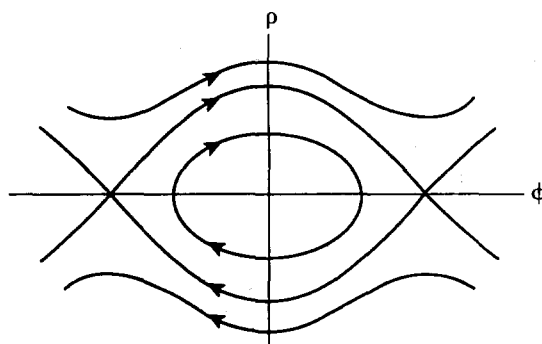


Fig. 3. The familiar phase space plot for a plane pendulum.

through a never ending succession of 2π rotations. But let us focus on the curve which lies at the border between these two types of motion. Here the pendulum departs its uppermost point of unstable equilibrium only to asymptotically return to that self-same position. Intuition immediately tells us that the smooth joining of the departing segment to the arriving segment is wildly improbable, for the final asymptotic return is equivalent to balancing a pencil on its point.

Integrable systems are rare first because their potentials must be such as to cause the smooth joining of departing and arriving curves for every unstable equilibrium point and second because such joining is an extremely difficult feat in a noisy world. The net effect of even the slightest perturbation is to cause the departing curve to intersect the arriving curve at nonzero angle, which, as Poincaré recognized, is a signature of nonintegrability. Moreover, even the slightest perturbation can increase the zero intersection angle of an integrable system; however, a finite perturbation is required to bring a finite angle to zero. Consequently, non-integrable systems are dense in C_k -space; equally, each nonintegrable system is surrounded by at least a small neighborhood in C_k -space devoid of integrable systems. Therefore one cannot, in general, approximate arbitrarily well the behavior of a nonintegrable system via judicious choice of an integrable system. On the other hand, in that rare circumstance when a nonintegrable system does lie near an integrable one, the behavior of the two will appear identical until computer accuracy exposes the difference.

With these results in hand, we can now appreciate why widespread integrability among the FPU systems would represent a coincidence so fortuitous as to border on the miraculous. Granted, any one FPU system, such as that in fig. 1, might be integrable, but FPU investigated many systems having distinct quadratic, cubic, or broken linear force laws, always obtaining results similar to those shown in fig. 1. Thus, although the FPU systems may be close to being integrable, in some sense, they are most certainly not all precisely integrable. But if they are not integrable, into what category do they fall? Because of a theorem he had proven some decades earlier, Fermi believed that FPU systems fell in the *ergodic* category. Recall that we are here discussing conservative systems whose orbits all lie on energy surfaces. A system is said to be *topologically ergodic*^{*)} on an energy surface provided provided almost all system orbits are everywhere dense on that energy surface. The notion of *metric ergodicity*^{*)} (on an energy surface) is more stringent and requires that all measurable sets, invariant under the dynamical flow, have measure zero or one. Metric ergodicity implies the physical definition^{**)} of ergodicity, which may be written

$$\lim_{t \rightarrow \infty} t^{-1} \int_0^t d\tau G[q_k(\tau), p_k(\tau)] = \int_E dq_k dp_k G(q_k, p_k). \quad (3)$$

Reading from left to right, eq. (3) asserts that time average of a function $G[q_k(t), p_k(t)]$ equals its phase space average taken over an energy surface. To summarize, Fermi believed that the time evolution of FPU systems should be such as to render states of equal energy equally likely. But in view of the FPU computer results, what deceived Fermi into thinking that weakly nonlinear oscillator

^{*)} A dynamical system is said to be *topologically ergodic* if all its orbits are dense on the energy surface, excepting perhaps an orbital set having measure zero. A dynamical system is said to be *metrically ergodic* provided the only measurable invariant sets on the energy surface have measure zero or one. Less technically, metric ergodicity means that the energy surface cannot be divided into two nonzero regions such that orbits always remain in their respective regions.

^{**)} Consult any good statistical mechanics text, e.g., ref. [6].

systems could be ergodic? In order to illuminate this point, we must first discuss Poincaré’s celebrated theorem on constants of the motion.

Poincaré sought to discover why, for an isolated system with N degrees of freedom, the energy occupies such a privileged position among the $(2N - 1)$ available constants of the motion. He elected to consider the quite general set of analytic Hamiltonians given by $H = H_0(P_k) + \mu H_1(Q_k, P_k)$, where H_0 is integrable, μ is small, and where the unperturbed ($\mu = 0$) frequencies of the H_0 -motion, given by $\omega_k = \partial H_0 / \partial P_k$, are functionally independent. Under these conditions, Poincaré proves [14] using arguments we shall sketch in just a moment, that there exists no constant of the motion $\Phi(Q_k, P_k, \mu)$ analytic in Q_k, P_k , and μ other than the energy H itself. Alternatively stated, the perturbation μH_1 in general “destroys” and does not continue the N analytic constants of the motion which exist for the integrable H_0 . Using precisely the same assumptions as Poincaré, Fermi later presented a proof that the above set of Hamiltonians would in general be ergodic. But are the FPU Hamiltonians, in fact, of the Poincaré type?

Now it is certainly true that the FPU Hamiltonians have the Poincaré form $H = H_0 + \mu H_1$, but the frequencies ω_k of the integrable harmonic oscillator Hamiltonian H_0 are constants and therefore not functionally independent. Nonetheless, there does exist a canonical transformation, whose exact form need not concern us here, for which the transformed FPU Hamiltonians may be shown to satisfy all the Poincaré conditions. Thus, the contradiction is real. Theory states that the FPU systems should under no circumstance exhibit the behavior revealed by the computer. To resolve this conflict, let us examine the theorems of Poincaré and Fermi in a bit more detail.

Poincaré starts with Hamiltonians of the type $H = H_0 + \mu H_1$. He then seeks constants of the motion of the form

$$\Phi(q, p, \mu) = \sum_{k=0}^{\infty} \mu^k \phi_k(q, p),$$

where q and p denote all position and momentum variables and where all $\phi_k(q, p)$ are analytic functions of q and p . Specifically, since Φ is a constant of the motion, he inserts the above expressions for H and Φ into the Poisson bracket equation $[H, \Phi] = 0$ and then insists that the coefficient of each μ^k equal zero. This procedure yields $[H_0, \phi_0] = 0$ at zeroth order and $[H_0, \phi_k] = -[H_1, \phi_{k-1}]$ for all $k > 0$, a set of equations which can be solved sequentially for all ϕ_k once ϕ_0 is specified, where ϕ_0 of course is any arbitrary constant of the motion for H_0 . The Poincaré procedure thus seeks to analytically continue ϕ_0 to nonzero values of μ . The proof that this continuation is impossible in general is straightforward but quite lengthy. Here, we confine ourselves to illustrating the crucial element in the proof. If, for example, we seek to continue the constant of the motion $\phi_0 = p_1^2$, we typically encounter terms which have frequency denominators of the type illustrated by

$$\Phi = p_1^2 + \mu \frac{q_1^2 p_2}{2\omega_1(p_k) - \omega_2(p_k)} + \dots, \quad (4)$$

where $\omega_l(p_k) = \partial H_0(p_k) / \partial p_l$. The denominator in eq. (4) is zero along some hypersurface in phase space. Moreover, in general a countable infinity of frequency denominators $\sum m_k \omega_k$ will appear in higher order which are zero along a dense set of hypersurfaces in phase space. But an analytic function cannot be infinite at a dense set of hypersurfaces; in consequence, no analytic constant of the motion exists, in general, other than the obvious: any function of H itself. The above is but one example of the

ubiquitous small denominators which, as Poincaré has shown, make the divergence of astronomical perturbation series the general case. Although numerous papers have appeared over the past ninety years claiming to circumvent or eliminate the small-denominator problem, small denominators represent *physical, nonlinear resonances* between degrees of freedom. They are innate and cannot be eliminated or circumvented; indeed, they are intimately connected with chaos^{*)} as we show later.

Fermi's proof [5, 6] that Hamiltonian systems are, in general, ergodic is based on Poincaré's nonexistence theorem. Specifically, Fermi begins by assuming that the Poincaré systems are not ergodic. In consequence, at least two distinct, nonzero regions invariant under the Hamiltonian flow in phase space must exist. Fermi now asserts that this fact implies the existence of an analytic, orbit bearing surface which separates the invariant regions. In turn, the existence of this surface implies the presence of an analytic constant of the motion for the Hamiltonian H , contrary to Poincaré's theorem. Fermi therefore concludes that the Poincaré systems are, in fact, ergodic.

Poincaré's theorem has withstood the scrutiny of nine decades; it is Fermi's theorem which contains the flaw. Nonetheless, Fermi's error reflects thinking typical of all physicists prior to 1950. Fermi therefore quite forgivably assumed that the dividing surface between invariant sets was analytic because the behavior of all the well-known physical systems exhibited precisely this behavior. In fact, it was not until the announcement by Kolmogorov in 1954 of what is now called the KAM theorem [15] that physicists were forced to abandon their notions of smooth analyticity. Expressly, KAM prove that the invariant regions for most Poincaré systems are disjoint sets which fill most of the allowed phase space, not surprisingly therefore, the surfaces separating these invariant regions obviously are intricately complicated, nonanalytic entities. Further details regarding the KAM theorem will appear later. But recognition of Fermi's error does not provide resolution of the basic issue. For, if ergodicity as well as higher forms of chaos does not reside in nonlinear oscillator systems, then where does it "hang out"? We begin our slow walk toward the answer to this question with a discussion of various attempts to explain FPU via integrable approximation.

3. Integrable approximations

In the late 50s, the present author sought to explain [16] the lack of equipartition revealed by the FPU systems. I argued that the FPU degrees of freedom could exhibit widespread energy sharing only if all were resonantly coupled. But in order for the weak resonant couplings in the Hamiltonian to be effective, the harmonic frequencies given by $\omega_k = 2(K/M)^{1/2} \sin(k\pi/2N)$ would have to obey resonant conditions of the form $\sum m_k \omega_k \approx 0$. But for the FPU ω_k -set, precise resonant conditions $\sum m_k \omega_k = 0$ are satisfied if and only if all the $m_k = 0$. Strictly speaking, this is true provided N is prime or a power of 2, the only values used by FPU. For other values of N , although a few resonant frequency conditions are satisfied, the FPU couplings fail to excite even these. Indeed, the only influential resonances are the approximate ones which occur along the small-argument, "straight-line" portion of $\sin(k\pi/2N)$ where $\omega_1 \approx \omega_2/2 \approx \omega_3/3 \approx \dots \approx \omega_k/k \approx \dots$, with the approximation becoming poorer as one reads to the right. Moreover, it is precisely these decreasingly effective resonances which are responsible for the energy sharing that occurs in decreasing amounts as mode number in fig. 1 increases. Thus far, my

^{*)} At this point, the reader is free to regard chaos as meaning little more than erratic, disordered, seemingly unpredictable. However, we perhaps should note that a system whose orbits are chaotic over its entire energy surface is both ergodic and mixing, where a system is said to be mixing if every small cell in phase space evolves into an increasingly thin filament which spreads uniformly over the entire energy surface.

arguments have involved only the physical notion of resonance without any hint of integrable approximation; they would therefore be expected to contain a substantial amount of truth. But then seeking analytic support, I resorted to integrable approximation in the form of a very primitive, divergent perturbation technique which, at least to a mother’s eye, gives semi-qualitative agreement with the FPU calculations – compare my fig. 4 with FPU’s fig. 1.

These results, first published in 1961, came as something of a surprise to various of my colleagues who, unbeknownst to me, were diligently polishing their own explanations of FPU. Consequently, they were not shy in exposing the glaring defects in my explanation. They were most troubled by my use of the unperturbed harmonic FPU frequencies when, in their view, the FPU perturbations were so large that only the perturbed frequencies could be relevant. As response, in 1963 I published a paper [17] which transformed certain of the FPU Hamiltonians to normal mode coordinates and then treated the unperturbed frequencies ω_k as free parameters. Figures 5a, b compare the standard FPU system for $N = 5$ with the “same” system whose unperturbed frequencies have been slightly shifted. Bringing the unperturbed FPU frequencies “on resonance” provides a dramatic increase in energy sharing. So much for the insignificance of unperturbed frequencies. Regardless, it was Freeman Dyson who provided the most penetrating comment, “Ford’s explanation cannot be regarded as the complete answer”. Indeed, Dyson’s comment applies equally well to all efforts at integrable approximation, as will become apparent in the sequel.

Also in 1963, E. Atlee Jackson [18] used a classical perturbation approach on the FPU systems which was similar to quantal Wigner–Brillouin perturbation theory. Specifically, the denominators in Jackson’s calculations involve the perturbed frequencies rather than the unperturbed frequencies used in my computations. This modification yields significantly improved agreement with the FPU computer results – compare Jackson’s theoretical predictions of fig. 6 with the FPU numerical results of fig. 1. Not only are Jackson’s normal mode curves approaching the correct shape, but the recurrence time is also being approached. Jackson’s results thus make it extremely clear that the FPU systems are, in fact, near an integrable system, but his series are nonetheless just as divergent as mine. Moreover, contact has not yet been made with Siegel’s theorem or Poincaré’s theorem. On that note, we turn to the last and by far the most renowned of the integrable approximations.

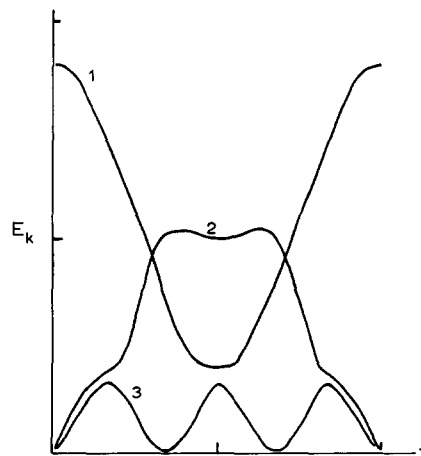


Fig. 4. The time evolution of the first three modal energies for the $N = 32$ FPU system of fig. 1 but here computed using a rather crude classical perturbation theory. The agreement is at best qualitative.

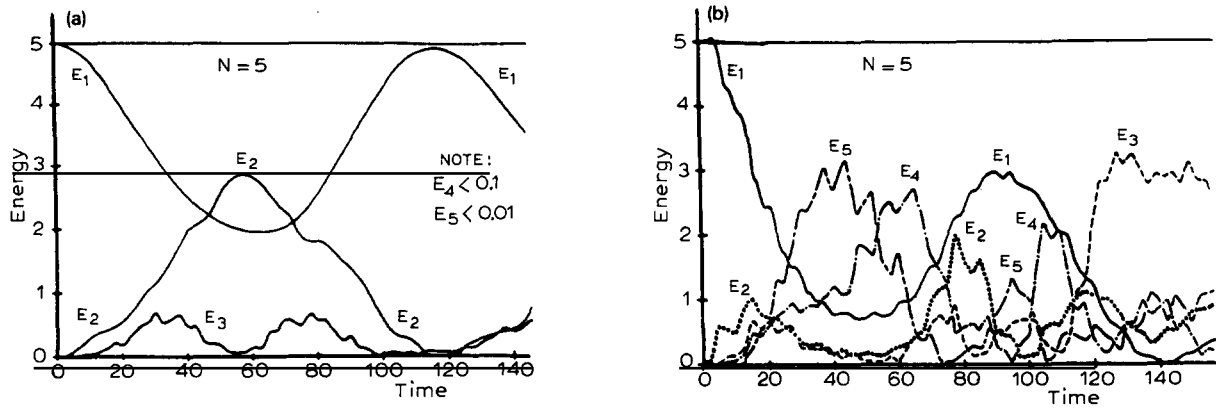


Fig. 5. These figures present a comparison of energy sharing as it occurs in two, closely related five-particle systems. (a) The modal energy curves for an $N = 5$ FPU system. Here one notes the typical decrease of modal energy as mode number increases. (b) Modal energy sharing of the "same" system as that in (a) except that for it the $N = 5$ FPU modal frequencies have been shifted slightly to bring them onto precise resonance. The increase in energy sharing is quite dramatic, emphasizing that the lack of wholesale energy sharing in the FPU systems is heavily influenced by the absence of internal resonances among the unperturbed FPU harmonic modal frequencies.

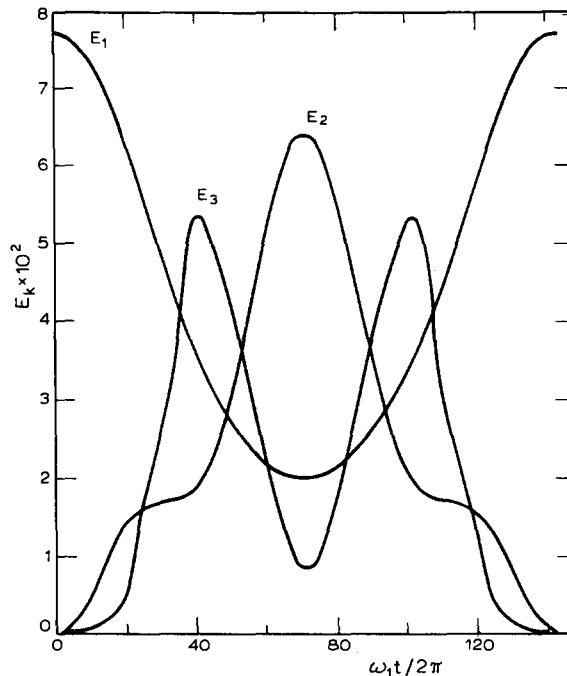


Fig. 6. An improved perturbative calculation for the time evolution of the modal energies for the $N = 32$ FPU system of fig. 1 obtained by Jackson [18]. Comparing this graph with that of fig. 1, one perceives the existence of at least semi-quantitative agreement between numerical and analytical results. Indeed, one now anticipates that a sufficiently sharpened perturbation theory could provide a quite accurate solution to the FPU problem.

For several years, Martin Kruskal and Norman J. Zabusky had sought a continuum approximation to FPU [19]. They began by noting that the normalized equations of motion for the FPU system of eq. (1) may be written

$$\ddot{Q}_k = (Q_{k+1} - 2Q_k + Q_{k-1}) + \alpha[(Q_{k+1} - Q_k)^2 - (Q_k - Q_{k-1})^2] \quad (5)$$

$$= (Q_{k+1} - 2Q_k + Q_{k-1})[1 + \alpha(Q_{k+1} - Q_{k-1})]. \quad (6)$$

In the lowest-order continuum limit, eq. (6) takes the form

$$Q_{tt} = Q_{xx} + \varepsilon Q_x Q_{xx} = (1 + \varepsilon Q_x) Q_{xx}, \quad (7)$$

where subscripts denote the usual partial derivative notation. But now eq. (7) may be viewed as just an ordinary wave equation whose wave speed c depends on its spatial derivative Q_x , i.e., $c^2 = (1 + \varepsilon Q_x)$. Typical behavior generated by eq. (7) for positive ε is seen in fig. 7, where an initial asymmetric pulse propagates to the right until its leading edge develops a vertical shock front, at which point eq. (7) loses validity. Nonetheless, prior to formation of the shock, eq. (7) provides a quite reasonable description of the FPU modal behavior. Kruskal–Zabusky (K–Z) thus sought ways to avoid the shock formation. In many physical systems, shocks are prevented by introducing dissipation; indeed, its inclusion leads to the so-called Burgers equation. Since FPU is conservative, K–Z elected to eliminate shock formation by introducing dispersion into the eq. (7) approximation to FPU. Specifically, they wrote

$$Q_{tt} = Q_{xx} + \varepsilon Q_x Q_{xx} + \beta Q_{xxxx}. \quad (8)$$

For both convenience and simplicity, K–Z now insist on periodic boundary conditions, restrict their attention to waves traveling in one direction only, and elect to sit in a frame moving with normalized speed $c = 1$. After replacing x by $\sigma = x - t$, t by $\tau = \varepsilon t$, Q_x by $U = \frac{1}{2} Q_x = \frac{1}{2} Q_\sigma$ in eq. (8), and neglecting terms proportional to ε^2 , they obtained the celebrated Korteweg–deVries (KdV) equation

$$U_\tau + UU_\sigma + \delta^2 U_{\sigma\sigma\sigma} = 0, \quad (9)$$

which is now known to be a completely integrable partial differential equation, meaning that eq. (9) can be derived from a Hamiltonian that is a function of its momenta alone.

K–Z then numerically integrated eq. (9) using periodic boundary conditions and one cycle of a cosine as initial condition. Much to their surprise, the initial cosine shape evolved into a finite number of relatively sharp pulses – see fig. 8 – that moved at distinct speeds about their periodic path like

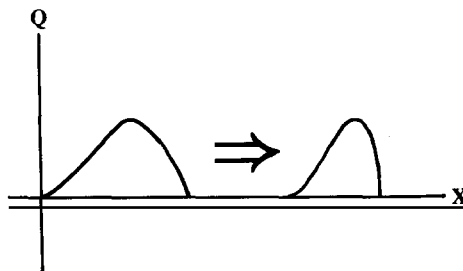


Fig. 7. This rough sketch shows an initial, asymmetric pulse time evolving to the right until its leading edge develops a vertical slope.

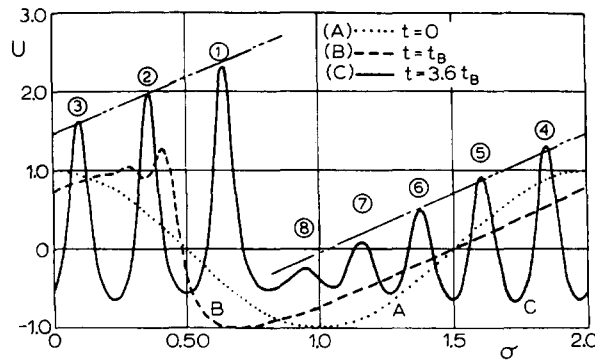


Fig. 8. The numerically integrated solution of the KdV equation for an initial condition taken as one period of a cosine, which here appears as the dotted curve. The shape of the time-evolved curve at a later time is shown as the dashed curve. Finally, the solid curve reveals that the initial cosine excitation has broken up into eight solitons which move with speeds proportional to their heights. The various FPU recurrences now find their explanation in terms of the recurrences which occur as these eight solitons move with incommensurate speeds around a circle.

runners on a track. Upon “collision”, the pulses would exhibit a nonlinear superposition during overlap and then all would emerge unchanged in shape or speed. The almost-periodic behavior of the FPU systems could now be understood at an especially clear, intuitive level. The first full recurrence of the FPU motion occurs when all the pulses approximately overlap, generating a near-return to the initial cosine shape. At half-recurrence, the pulses overlap in two distinct groups forming the second harmonic shape, at one-third recurrence, three distinct groups of pulses overlap, etc. For long-wavelength excitations where the continuum approximation might be expected to provide reasonable results, approximating FPU by KdV provides qualitative to quantitative agreement, depending on the quantity being considered. However, if one wishes to approximate the modal curves of fig. 1, the Jackson series yield results comparable to and perhaps better than those of K–Z. For short-wavelength initial conditions, the K–Z approach is, of course, simply not applicable. Therefore, in regard to the FPU problem, KdV is highly ingenious and delightfully intuitive, but in the end it is nothing more than another integrable approximation.

However in the process of developing their explanation of FPU, Kruskal and Zabusky were led to provide insight into a much larger class of problems. Indeed, they were the first who turned the FPU paradox into discovery, for the pulses mentioned just above are, in fact, the celebrated K–Z solitons, now found to be ubiquitous in nature, while the KdV equation has become the paradigm for an expanding class of completely integrable nonlinear partial differential equations. Over the years, the terms inverse scattering, Lax pairs, breathers, kinks, soliton–antisoliton pairs, and the like have become household words in mathematical physics, reflecting but a part of the “industry” founded by Kruskal and Zabusky. All these matters have been covered in such detail at countless conferences and in review articles beyond number that almost nothing remains unconsidered. However, there are perhaps a couple of significant yet frequently overlooked points worthy of mention. Specifically, why is the soliton so ubiquitous and why does it occur at all?

The following discussion is intended to provide an intuitive understanding of only the K–Z soliton, why it occurs and why it is observed in so many physical systems; readers desiring to know more about the zoology of contemporary solitons are referred to the vast literature which exists on this topic. Consider now the innocent looking one-dimensional array of equi-spaced, equi-mass points sitting at rest in fig. 9a, where the leftmost mass, labeled 1, has just been given a velocity \mathcal{V} to the right. Upon

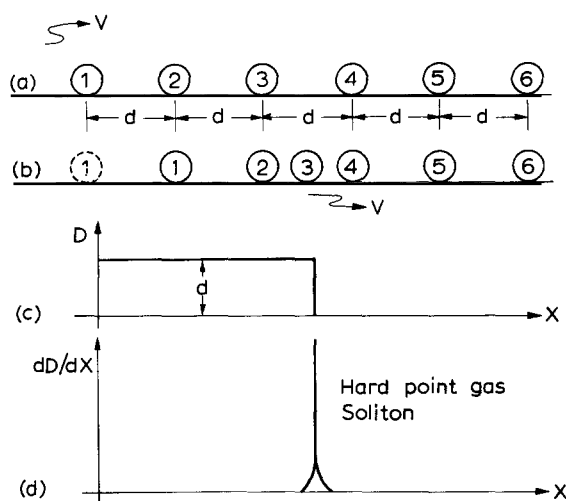


Fig. 9. (a) An array of equal mass coins sitting at rest until the leftmost coin is given a velocity \mathcal{V} to the right. (b) The situation after particle one has collided with two, two with three, and three is headed toward four. (c) The sequential displacement of particles one step to the right may be represented by the right moving square wave of displacement shown here. (d) Finally, by taking the derivative of the square wave shown in (c) as is customary in soliton theory, the most primitive of all solitons is revealed; the soliton is here seen to result from nothing more than a hard-core interaction.

colliding with mass 2, mass 1 comes to rest at the original position of 2, while 2 moves off with velocity \mathcal{V} to the right; 2 then comes to rest at the position of 3 as 3 heads with velocity \mathcal{V} toward 4. Figure 9b shows this latter situation for comparison with that of fig. 9a. One may describe this motion as essentially that of a square wave moving to the right. Actually, the leading edge of the wave is not vertical but sloped; however, this discrepancy disappears at large \mathcal{V} and/or small interparticle spacing. In the notation of eq. (8), the square wave $Q(x)$ appropriate to fig. 9b appears in fig. 9c. Finally, by taking the derivative $U = Q_x$ invoked by the K–Z theory, we easily obtain the δ -function of fig. 9d, which exposes the primitive, archetypical essence of the soliton. Indeed, the soliton is here clearly revealed to be a hard-core, billiard ball, knock-on rowdy. Without the hard-core interaction, or at least an asymmetry in the pair potential, the K–Z soliton cannot exist. The billiard ball analogy makes it clear that this soliton is a localized excitation only in one dimension, although there can be plane wave solitons in two and three dimensions.

Finally, we at last have no trouble recognizing that the soliton is as ubiquitous as hard-core interactions. But now the inverse question arises: if they are so common, why were not solitons discovered centuries ago? The answer is, in fact, quite astonishing, but depth psychology lies beyond the scope of this article. Instead, let us move toward the land where solitons decay, integrable approximations falter, and the laws of chance reign supreme.

4. The transition to chaos^{*})

When the FPU calculations failed to exhibit the expected chaos, there was no scarcity of people offering ready explanations. Of these, the argument that the FPU force laws were too simple lost

^{*}) We now enlarge the meaning of chaos to include the notion of exponentially sensitive dependence of final state upon initial state, which implies that two initially close phase space states separate exponentially with time. It also implies that the slightest imprecision in the present state fogs a system's memory of its distant past and vision of its distant future.

credibility when Northcote and Potts [20] found statistical behavior in a one-dimensional array of harmonically coupled hard rods. The notion that the FPU recurrence might simply be a Poincaré recurrence was demolished by the estimates of Hemmer et al. [21] who established that the relevant Poincaré times increase exponentially with particle number N while the FPU recurrence times grow like a power of N . The suggestion that one-dimensional systems are poor candidates for chaos runs afoul of the positive results obtained by Casati et al. [22] who demonstrated that 1-D systems can, in fact, exhibit a normal Fourier thermal conductivity. One of the more persistent beliefs held that the thermal relaxation times for the FPU systems were too long to be observed during the short integration runs made by FPU; big Jim Tuck and Mary Menzel (née Tsingou) [23] buried this conjecture under many hours of numerical computation – a sample is shown in fig. 10. Finally, many researchers had begun to suspect that the impressive success of integrable approximations meant FPU would eventually be shown to be integrable. Let us now dispel this last illusion by exposing an FPU transition to chaos.

Consider a three-particle FPU system having periodic boundary conditions which is governed by the Hamiltonian

$$H = \frac{1}{2} \sum P_k^2 + \frac{1}{2} \sum (Q_{k+1} - Q_k)^2 + \frac{\alpha}{3} \sum (Q_{k+1} - Q_k)^3, \tag{10}$$

where all sums run from $k = 1$ to 3 and where $Q_4 \equiv Q_1$. After introduction of a canonical change of variables to harmonic normal mode coordinates $(\mathcal{Q}_k, \mathcal{P}_k)$, Hamiltonian (10) takes the form

$$\mathcal{H} = \frac{1}{2} (\mathcal{P}_1^2 + \mathcal{P}_2^2 + \mathcal{P}_3^2) + \frac{1}{2} (3\mathcal{Q}_2^2 + 3\mathcal{Q}_3^2) + (3\alpha/\sqrt{2})(\mathcal{Q}_2\mathcal{Q}_3^2 - \frac{1}{3}\mathcal{Q}_2^3). \tag{11}$$

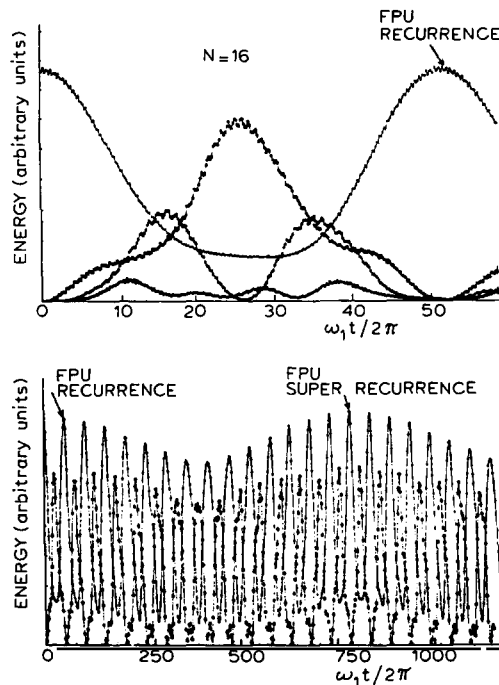


Fig. 10. In the upper part of this figure is seen the standard energy sharing between normal modes for an FPU system (here $N = 16$) integrated through one recurrence. By greatly extending the integration interval as shown in the lower figure, Tuck and Menzel [23] exposed a superperiod of recurrence. Their calculation leaves little doubt regarding almost-periodicity in the FPU motion.

Note that the coordinate \mathcal{Q}_1 locating the center of mass is absent from \mathcal{H} , implying that the center of mass moves with constant momentum \mathcal{P}_1 . Thus, transforming to the center of mass frame and setting $t = \tau/\sqrt{3}$, $\mathcal{Q}_2 = (\sqrt{2}/\alpha)q_2$, and $\mathcal{Q}_3 = (\sqrt{2}/\alpha)q_1$, we obtain

$$H = \frac{1}{2}(p_1^2 + p_2^2 + q_1^2 + q_2^2) + q_1^2 q_2 - \frac{1}{3}q_2^3. \quad (12)$$

But Hamiltonian (12), which is canonically equivalent to the FPU system of eq. (10), is the celebrated Hénon–Heiles Hamiltonian [24], whose chaotic properties have been exhaustively investigated. Therefore, as we now review the chaotic behavior exhibited by the Hénon–Heiles system, we are simultaneously exposing the chaos hidden from view in the original FPU results.

Hénon and Heiles studied the global behavior of orbits for the bounded motion of Hamiltonian (12) via a Poincaré surface of section constructed as follows. Clearly, an orbit for Hamiltonian (12) must be viewed as lying in a four-dimensional (q_1, q_2, p_1, p_2) space. Yet because the energy $H = E$ is a constant of the motion, orbits can in fact be drawn in a three-dimensional (q_1, q_2, p_2) space, for, once q_1, q_2, p_2 are given, then $p_1 \geq 0$ (or $p_1 < 0$) is uniquely determined by $E = E(q_1, q_2, p_1, p_2)$. But now note that the (q_2, p_2) plane provides a cross section – a plane Poincaré surface of section – of this (q_1, q_2, p_2) space. Hence, we may obtain a global picture of orbital behavior at each energy by determining each orbit’s intersection points with the (q_2, p_2) plane, i.e., (q_2, p_2) points on an orbit at which $q_1 = 0$ and (to remove ambiguity) $p_1 > 0$. Now, were the Hénon–Heiles system chaotic with no constants of the motion other than the total energy, then the (q_2, p_2) plane intersection points for each orbit would be expected to form an erratic splatter with no apparent pattern. On the other hand, if the Hénon–Heiles system were integrable having an analytic constant of the motion $\Phi = \Phi(q_1, q_2, p_1, p_2)$ in addition to the energy, then by solving the energy E for $p_1 > 0$ and thence placing this p_1 into Φ , one finds $\Phi = \Phi(E, q_1, q_2, p_2)$, an equation for a two-dimensional surface embedded in a three-dimensional (q_1, q_2, p_2) space. But now by setting $q_1 = 0$ in Φ , we may determine the analytic curves $\Phi = \Phi(E, q_2, p_2)$ in the (q_2, p_2) plane upon which the orbital intersection points must lie. Thus, no matter whether integrable or chaotic, Hénon–Heiles had only to numerically integrate the orbits of Hamiltonian (12), determining (q_2, p_2) intersection points, in order to establish the character of the system motion at each desired energy value. As the energy grows the cubic nonlinear terms in eq. (12) increasingly perturb the harmonic quadratic terms. Thus, Hénon–Heiles use energy as their perturbation parameter.

Figure 11 shows the (q_2, p_2) Poincaré surface of section at energy $E = 1/12$ for the Hénon–Heiles Hamiltonian (12). Here, curves seem to exist everywhere, indicating the possibility of an additional constant of the motion and the integrability of Hamiltonian (12). Note that each curve in fig. 11 is made up of intersection points generated by a single orbit. But now what happens if the energy is increased, permitting the nonlinear terms in eq. (12) to grow in size relative to the linear ones? Figure 12 at $E = 1/8$ provides the answer. Curves persist in the neighborhood of the stable fixed points along the q_2 and p_2 axes (corresponding to periodic orbits), but a region of erratic dots appears between these stable areas. In fact, all the orbits in this region generate a diffuse spray of points. Moreover, throughout this region two close initial conditions yield orbits whose separation distance grows exponentially with time whereas separation distance for integrable systems exhibits power law growth. Turning now to fig. 13, we see that the small apparently random array of orbital intersection points in fig. 12 has grown to fill almost all the available area at energy $E = 1/6$. The complete “order” of fig. 11 has now turned into the complete “chaos” of fig. 13. With these three simple figures, Hénon–Heiles banished forever the clockwork universe popularized centuries earlier by Laplace. Indeed, the elegant simplicity and the

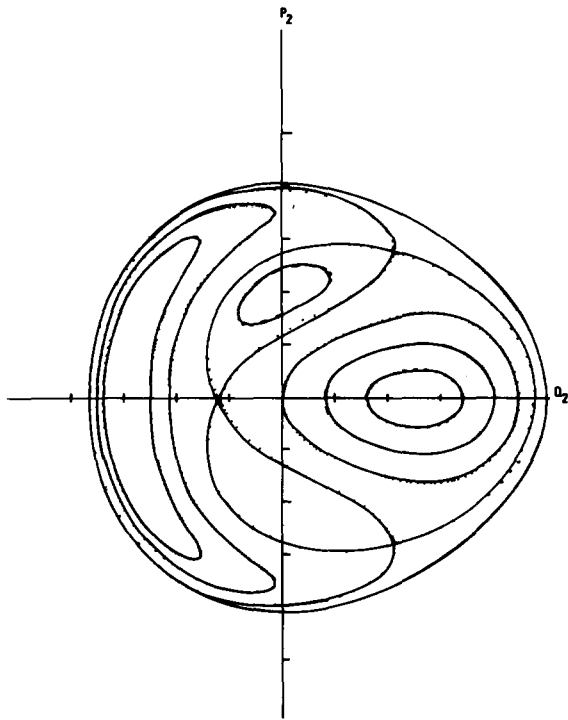


Fig. 11. The first of three figures which originally appeared in the celebrated paper by Hénon and Heiles [24]. Here we see a plot of the Poincaré surface of section for the Hénon–Heiles conservative system at system energy $E = 1/12$. Curves appear to exist everywhere in the permitted area, indicating possible integrability.

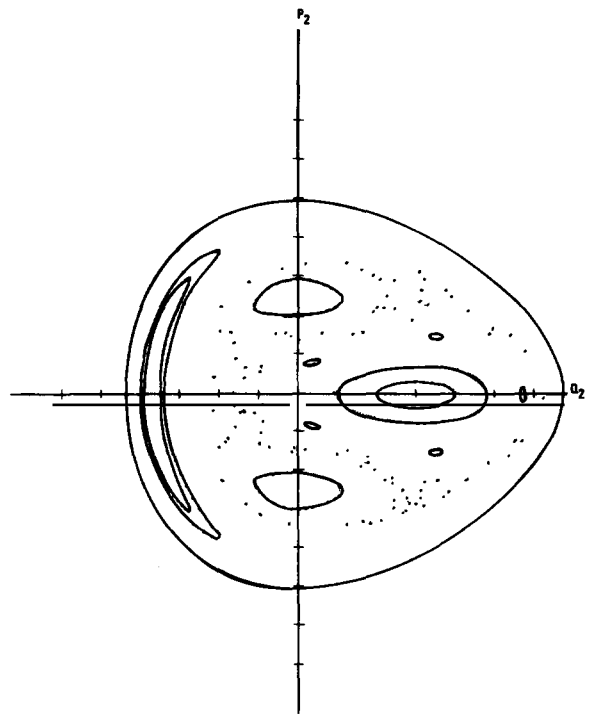


Fig. 12. The genuine surprise provided by the Hénon–Heiles calculations first appeared in this figure for $E = 1/8$. All this “random splatter” of dots was generated by a single orbit. All hope of integrability now disappears. Indeed, since Hénon and Heiles demonstrated the sensitive dependence of orbits lying in this “splatter” region, this figure provides an early illustration of the transition to chaos in a Hamiltonian system with only two degrees of freedom.

convincing clarity of the evidence for a transition to chaos in their two-body system has made the Hénon–Heiles paper the most frequently quoted work in all nonlinear dynamics/chaos. But let us not forget that the chaos of Hamiltonian (12) is also the chaos of the FPU Hamiltonian (10), and that the transition to chaos seen in figs. 11–13 is also the transition to chaos veiled by the FPU calculations.

Confronted with the chaos occurring at the higher energies for Hamiltonian (12), a number of investigators turned to integrable approximations in the hope that their failure might become obvious at or near the transition to chaos, but of course, such methods cannot describe chaos itself. In this regard, it is, in retrospect, perhaps a tribute to Laplace that those who invoked integrable approximations to describe FPU were content to look no further. But regarding Hénon–Heiles, perhaps the most illuminating study based on an integrable approximation was that conducted by Gustavson [25], who used the elegant perturbation theory of Birkhoff [4] to compute a power series in q_k and p_k (calculated to eighth order) for an additional constant of the motion. In the Gustavson–Birkhoff procedure, the perturbation parameter is neither Poincaré’s μ nor Hénon–Heiles’ E ; it is rather the order of the terms in the power series expansion, which are assumed to decrease in size as the order increases. The additional constant of the motion Gustavson obtained permitted him to obtain analytic (q_2, p_2) surface of section plots. His entire approach was, of course, feasible only because large computers could perform the lengthy symbol manipulations in a reasonable time interval. Gustavson’s comparison of

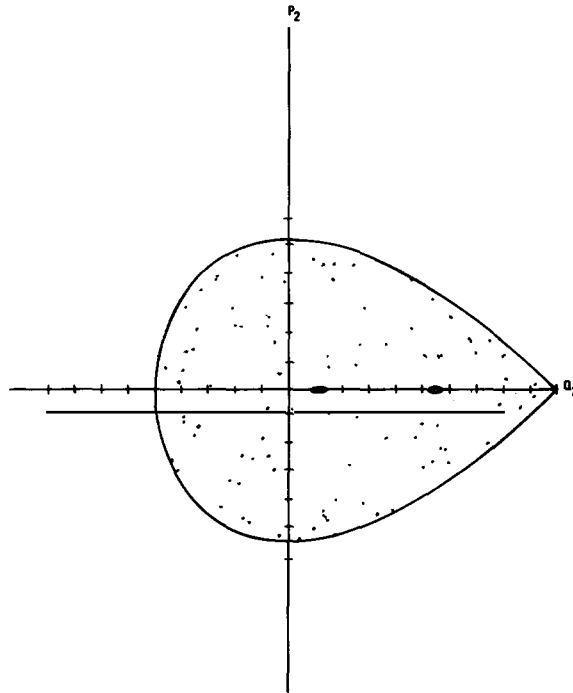


Fig. 13. This Poincaré surface of section at system energy $E = 1/6$ provides icing on the cake showing that the system becomes almost totally chaotic slightly before the energy for unbounded motion is reached.

perturbation theory with numerical integration appears in fig. 14. The comparison is for energies $E = 1/12$, $1/8$, and $1/6$ as one would expect. Note that perturbation theory provides smooth curves at all three energies; disappointingly it thus gives not the slightest hint of its own failure, not even at the higher energies. In fact, though not apparent in fig. 14, perturbation theory cannot be truly accurate at any energy, for the Birkhoff power series constructed by Gustavson, despite the fact that it gives fair agreement at $E = 1/12$, has been shown to be not only divergent but apparently an asymptotic representation of a nonexistent constant of the motion! In order to remove a bit of the mystery from these remarks, let us present a brief outline of what is happening in both Hénon–Heiles and FPU. Details as well as rigor will be supplied later.

The Hénon–Heiles paper presented a graph showing the fractional amount of area in each surface of section containing smooth curves as a function of energy. To the accuracy of their calculations, a plot of this fraction initially moved along a horizontal line at the value one, but at about $E = 1/10$ the fraction began an abrupt fall toward zero along a rapidly descending straight line. The discontinuity near $E = 1/10$ lent support to the notion that chaos first appears at the discontinuity point. However, more accurate surfaces of section would have revealed a slow, smooth decrease in the curve bearing area from unity at $E = 0$ to almost zero at $E = 1/6$. Nonetheless, this smooth curve would be almost flat below $E \approx 1/10$ and would display a rapid falloff to zero as $E \rightarrow 1/6$. In short, both Hénon–Heiles and FPU appear integrable as long as chaos lies below the level of computer accuracy, but increasing energy (nonlinearity) finally broadens the chaos regions until they can be seen by even a low-precision computer.

Thus it was not integrating over too short a time interval which hid the chaos innate to the FPU

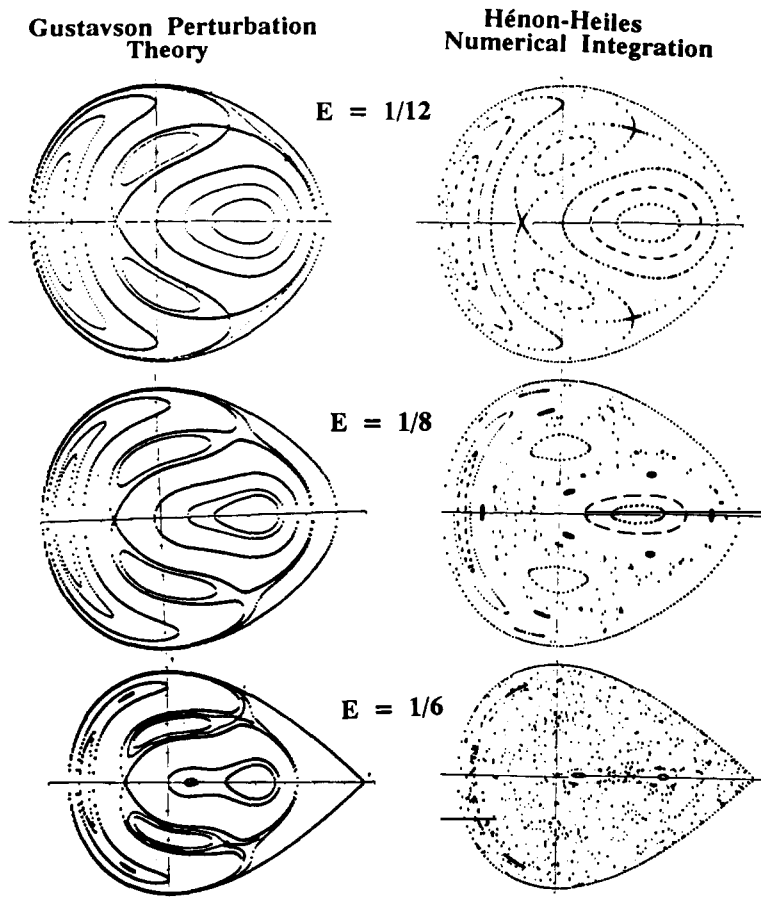


Fig. 14. After automating the required symbol manipulation on a computer, Gustavson [25] determined a power series expansion for a formal constant of the motion for the Hénon–Heiles system valid through eighth order. With this constant of the motion, Gustavson then computed analytic surface of section plots for comparison with the numerical integrations of Hénon–Heiles. The results are shown here. The agreement between Gustavson and Hénon–Heiles is quite satisfactory in all those regions where Hénon–Heiles find curves, elsewhere the analysis of Gustavson fails without warning.

systems but the lack of computer accuracy and/or the lack of sufficiently strong nonlinearity. But an inquisitive reader will surely wonder why the integrable approximations work so well at low to moderate energies and/or why the nonlinearity in the FPU Hamiltonian (10) [or the Hénon–Heiles Hamiltonian (12), for that matter] must become so large before its chaos becomes visible to a single-precision computer? When, as here, the Hamiltonians under consideration are of the form $H = H_0 + \mu H_1$, the uninitiated would most certainly expect the perturbed motion of H to closely resemble that of the unperturbed H_0 when μH_1 is relatively small. However, this expectation becomes less and less reasonable as μH_1 grows into the moderate range. Yet the FPU and Hénon–Heiles Hamiltonians still appear integrable for energies greater than our wildest expectations. Why? It can be immediately stated that the perturbed motion is not even close to that of the unperturbed harmonic oscillator H_0 of eqs. (11), (12). The surface of section for an independent oscillator $E = \frac{1}{2}(p^2 + \omega^2 q^2)$ would consist of circles about the origin. There is not a hint of such behavior in fig. 11 nor in fig. 15 at extremely low energy. We thus need a nonlinear Hamiltonian close to the two we consider. The

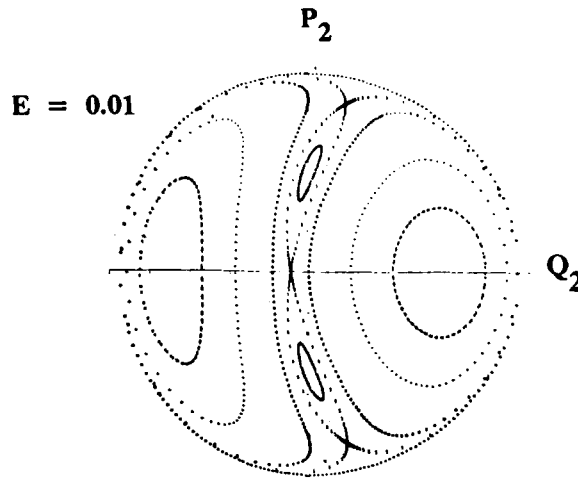


Fig. 15. In both the FPU and the Hénon–Heiles systems, the transition to chaos does not occur until the energy increases rather far away from zero. There must be some nearby integrable system causing this behavior, but it is most certainly not that of independent harmonic oscillators from which both FPU and Hénon–Heiles start at $E=0$, as is shown by this very low energy surface of section for the Hénon–Heiles system. Indeed, the oscillators shown in this figure are sharing energy.

nonlinear KdV equation is one respectable candidate. Another is the Hamiltonian which results after changing the very last sign in eq. (12); this renders eq. (12) both integrable and separable. Finally, perhaps the most attractive candidate of all is the three-particle, “exponential” Toda Hamiltonian [26]

$$H = \frac{1}{2} \sum P_k^2 + \frac{1}{2} \left(\sum e^{(Q_{k+1} - Q_k)} \right) - 3, \quad (13)$$

where the index k runs from 1 to 3 and where periodic boundary conditions imply that $Q_4 \equiv Q_1$. There is a legitimate sense in which the N -particle Toda system may be regarded as a discrete version of the KdV equation. Equation (13) is both integrable and exhibits K–Z solitons. Finally, if one eliminates the translation mode in eq. (13) and then expands the resulting two degrees of freedom Hamiltonian in a power series retaining terms only through third order, the FPU/Hénon–Heiles Hamiltonian of eq. (12) is obtained. If one eliminates the translation degree of freedom from eq. (13) but does not expand in a series, the resulting two degrees of freedom system yields surface of section plots which are only distorted versions of fig. 11. We cannot rule out the existence of a nonlinear integrable system closer to FPU/Hénon–Heiles than the Toda system, but it is perhaps close enough for our purposes.

Until now we have exposed only pieces of the FPU puzzle. Many questions have been answered but many yet remain. In a sense, a pattern has formed but a satisfying picture has not emerged. Thus, let us now complete the puzzle by adding one final unifying piece. Specifically, let us now focus our attention on a theorem announced without proof by A.N. Kolmogorov at the 1954 Conference of Mathematicians in Amsterdam, which, though no one noticed at the time, could have explained the lack of chaos observed by FPU a priori. But Kolmogorov’s theorem (see appendix D of ref. [27]), like the FPU preprint, attracted little notice in a busy world. Indeed, realization of the full significance of this theorem was further impeded by the extremely lengthy and highly technical independent proofs published by Arnol’d [28] in 1963 and by Moser [29] in 1962 some ten years after Kolmogorov’s original announcement. Moreover, many of that handful of physicists who took the time to cut through the

hedgerows of unfamiliar technical jargon concluded they were learning more about the convergence problems of celestial mechanics than they wanted to know. However, much, much more than the problem of small denominators in celestial mechanics was involved in what we now call the KAM theorem. Let us digress briefly to discuss this issue.

By the end of the last century, if not before, it was clear to any scientist who bothered to examine the matter that there were two quite contradictory views regarding the character of the motion for Hamiltonians $H = H_0 + \mu H_1$. One view assumed that the perturbation μH_1 serves only to add a “few harmonics” and slightly shift the frequencies of the H_0 motion, thereby justifying the use of standard perturbation theory. The other accepted the notions of statistical mechanics which assert that even the weakest μH_1 is sufficient to convert the integrable motion of H_0 to an ergodic motion in which states of equal energy are equally likely. Given such disparate views, it is amazing that no debate raged during the early decades of this century. In retrospect, it seems that this was a classic case of people in glass houses fearing to throw theoretical stones, because each side had only nonrigorous, a posteriori justification for their positions. Indeed, before KAM there was no rigorous answer to the question, “Under what circumstances does the motion of $H = H_0 + \mu H_1$ closely resemble the motion of H_0 ?” Moreover, the evidence accumulated over many decades prior to KAM, of which FPU is but a small part, seemed so contradictory that resolution was not seen even on a distant horizon. Nonetheless, work on the FPU part of the overall puzzle led Kruskal and Zabusky to discover the soliton and thence to found a whole new area of mathematical research. Moreover, the title of the present paper would have been even more appropriate had FPU served as motivation for the KAM theorem; unfortunately, the actual timing of events proves otherwise. But even so, while FPU did not directly influence KAM, they did much to prepare the fertile soil in which the KAM theorem and nonlinear dynamics/chaos eventually grew.

Given the above remarks as prologue, let us now state the KAM

Theorem. Given an analytic Hamiltonian $H = H_0 + \mu H_1$ satisfying the usual Poincaré assumptions, (i) H_0 is integrable, (ii) μ is sufficiently small, and (iii) $\det|\partial^2 H_0/\partial P_k \partial P_l| = \det|\partial \omega_k/\partial P_l| \neq 0$ (where $\omega_k = \partial H_0/\partial P_k$), then there exists a nowhere dense^{*)} set of H_0 tori which are only slightly distorted by the small μH_1 perturbation. Moreover, the measure^{**)} of this nowhere dense set of “preserved” tori is nearly that of the allowed phase space. The complementary set of “destroyed” H_0 tori is dense but has small measure.

With this theorem, KAM abandoned all hope of showing that every H_0 torus will, under the influence of μH_1 , simply distort into a perturbed torus of the full Hamiltonian, for they knew full well that the dense set of H_0 tori having all rational frequencies ω_k yield the sums $\sum m_k \omega_k$ that appear as the zero to small denominators – see eq. (4) – which cause the divergence of almost all perturbation series in classical dynamics.

^{*)} The closure $\text{cl}(A)$ of a set A is defined to be the union of the set A with all its limit points. A subset A of a set S is called dense in S if and only if $\text{cl}(A) = S$. The subset A is said to be nowhere dense in S if the complement of $\text{cl}(A)$ is dense there. To illustrate, let us delete all the rationals (h/k) from the unit interval plus a small interval $(2\epsilon/k^3)$ about each; the finite length of the deleted intervals is proportional to $\epsilon \ll 1$. This set of deleted intervals is dense; its complement is nowhere dense yet includes almost all the length of the unit interval.

^{**)} For continuous point sets, measure simply means length, area, volume, or the like. For discontinuous or disjoint point sets, we may cover such sets with a collection of lengths, areas, volumes, or the like. We may then determine the length, area, volume, etc., of the limiting collection of elements which just cover the given set, and we then call this the measure of the set. As illustration, we note that the rationals (h/k) in the above footnote can be covered by intervals $(2\epsilon/k^3)$ whose total length can be made as small as we please. We thus assert that this set of rationals has measure zero.

Thus, in order to salvage as much as possible from this crush of densely packed tori causing small denominators, KAM elect to perturb only those H_0 tori whose frequency sums satisfy $|\sum m_k \omega_k| \geq K/(\sum |m_k|)^\nu$, where $\nu > 2$ and K are positive real numbers independent of the integers m_k and the frequencies ω_k . This restriction deletes from phase space not only those H_0 tori having rational frequencies but a small neighborhood surrounding each “rational” torus as well. Nonetheless, a quite large majority of the H_0 tori remain, for, even though all tori in a $2\varepsilon(\sum |m_k|)^{-\nu}$ neighborhood of each rational torus having $|\sum m_k \omega_k|$ are deleted, these neighborhoods decrease as $\sum |m_k|$ increases in such a way that the deleted “volume” of phase space is proportional to ε . The parameter ε can be chosen as small as convergence requires and the perturbation coefficient μ permits.

But the elimination of all tori causing too small denominators is only the first step in achieving convergence of the KAM perturbation series; specifically, the numerators in their series must decrease more rapidly than do the higher-order denominators. KAM ensure such convergence by choosing an iterative-type procedure (Newton’s method) which provides a strong quadratic convergence of the numerators to zero.

Ordinarily, the error of perturbation schemes decreases like μ, μ^2, μ^3, μ^4 , etc., as the number of terms increases. On the other hand, the error in quadratically convergent schemes decreases like μ, μ^2, μ^4, μ^8 , etc., as the number of iterations increases. For example, the recursion formula $A_{n+1} = [(A_n^2 + 2)/2A_n]$ for computing $\sqrt{2}$ provides iterates in which the error in A_{n+1} is proportional to the square of the error in A_n . To illustrate, if we set $A_0 = 1.4$ then we find $A_1 = 1.414$, $A_2 = 1.41421356$, etc. Here, A_1 returns four accurate digits for two while A_2 returns eight accurate digits for four. In short, the iterates A_n deviate from $\sqrt{2}$ by an error which decreases like μ^{2^n} . This example is typical of the quadratic convergence which enables the KAM proofs.

But small denominators and quadratic convergence aside, what insights does the KAM theorem provide into the character of the motion for the Hamiltonian systems $H = H_0 + \mu H_1$? First, KAM at last reveal the conditions under which such systems may be called nearly integrable (Moser’s terminology). But they do so at the cost of introducing a pathology in phase space which is truly mind boggling, as we shall shortly illustrate. It is precisely this pathology of intermingled dense and nondense sets which make it obvious why Poincaré could, in general, find no constants of the motion other than the total energy and why classical perturbation series must diverge. But if now, with KAM, we focus on the nondense set of only slightly distorted tori in essence carrying the measure of the space, we perceive that convergent perturbation theories can be devised which are valid for most, though not all, initial conditions. Indeed, it is precisely some subset of preserved KAM tori that all the standard perturbation theories are approximating until increasing nonlinearity forces them into absurdity.

However, perhaps the deepest insights into the structure of phase space (energy surface) for KAM nearly integrable systems are provided by fig. 16b, due to Arnol’d, showing a Poincaré section for a generic, two degrees of freedom Hamiltonian system. For reference, fig. 16a shows a set of preserved nested tori as well as the surface of section used in fig. 16b. In fig. 16b itself, the origin at the center of the circles is most conveniently viewed as the isolated intersection of a stable periodic orbit with the surface of section shown in fig. 16a, although it is possible to view it as a point of stable equilibrium.

Near the origin the perturbation is presumed weak. Here, the preserved KAM tori are too closely spaced to see the intervening structure. However, as our eye moves out from the origin, we observe, as Poincaré and Birkhoff [30] predicted, the alternating elliptic and hyperbolic points generated by the only periodic orbits to survive the destruction of an integrable torus bearing only periodic orbits. One periodic orbit is stable, being surrounded by elliptic invariant curves, each generated by a single trajectory. The other periodic orbit is unstable, being surrounded locally by hyperbolic invariant curves.

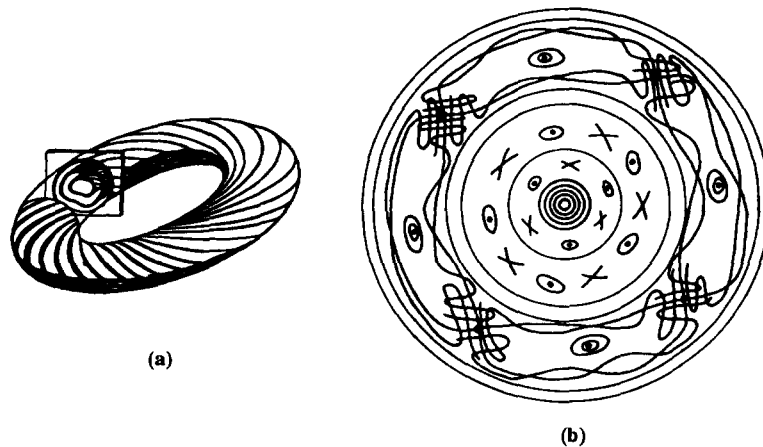


Fig. 16. On the left is seen a set of nested tori with a cutaway showing a Poincaré surface of section. An exploded view of this surface of section is shown on the right. The circles represent preserved tori. The first signs of instability are represented by the alternating elliptic–hyperbolic pairs surrounding the origin. Moving out from the origin, one sees intersecting invariant curves in whose neighborhood lie trajectories which are realizations of random processes. But the true complexity implied by this picture is that it is replicated about each elliptic fixed point in the figure and in each replication ad infinitum.

The additional elliptic–hyperbolic pairs which appear further out from the origin are generated by the same mechanism; the number of stable–unstable pairs is dictated by the ω_2/ω_1 ratio of periodic orbits on the original integrable torus. Just as was the case when the pendulum of fig. 3 was perturbed, the invariant curves departing and approaching the unstable hyperbolic points intersect and form an unbelievably intricate “lattice”. This mesh of intersecting curves is generated near all the hyperbolic points but is pictured in fig. 16b only near its boundary. Points generated by orbits passing through the neighborhood containing this mesh are wildly erratic and initially close orbits separate at an exponential rate. Moreover, as the size of the perturbation increases, these flailing invariant curves fan out and stir an increasing amount of phase space into an uncontrolled frenzy. Indeed, it is this behavior which is responsible for the erratic splatter seen in the Hénon–Heiles system. But we are only warming to the task of describing the complexity implied by fig. 16b, most of which cannot be drawn in this figure.

Specifically, the annular regions bearing alternating elliptic–hyperbolic pairs are dense throughout the figure [31]; moreover, the lattices formed by intersecting invariant curves occur, but of varying widths, in every neighborhood of the central invariant point [31]. Interior to each lattice region there is (at least) a countable infinity of orbits which cannot be distinguished from a realization of a random process. Moreover, the structure of fig. 16b is replicated around the center of every elliptic region in the figure. “The dog has fleas, who themselves have fleas, who in turn also have fleas . . .”

But in fig. 16b, the everywhere dense regions of erratic behavior are disjoint, being separated by the preserved KAM tori. However, when the system degrees of freedom are three or greater, the tori no longer divide the energy surface and orbits in the chaotic regions can spread over the entire energy surface undergoing a motion called Arnol’d diffusion [11]. This diffusion is exponentially slow but it might nonetheless be of importance in physical situations such as occur in colliding beam accelerators where particle bunches can collide an astronomical number of times during one experiment [12]. But perhaps more important, this almost universal Arnol’d diffusion represents that seed which grows into full blown chaos when the nonlinearity dominates.

Finally, looking again at fig. 16b, the complexity implied there is so great that Poincaré did not even attempt to draw it; specifically, he wrote, “One is struck by the complexity of this figure that I am not even attempting to draw. Nothing can give us a better idea of the complexity of the three-body problem and of all problems of dynamics where there is no holomorphic integral and Bohlin’s series diverge.”

It is precisely the dynamical pathology revealed by fig. 16b which was missed by all the integrable approximations to the Fermi–Pasta–Ulam problem. But in a deeper sense, fig. 16b in fact reveals the richness of dynamics, not its pathology. A growing nonlinearity removes the shackles imposed by analytic constants of the motion, permitting a system to explore its energy surface unfettered and free. The resulting erratic motion may be undisciplined but it is never dull. Currently, there has even appeared a first bud of realization that this motion may have practical applications [32].

Let us now return to FPU. Boris Chirikov [33–35] was the first to recognize that the input data used by FPU placed their systems squarely in KAM’s region of stability. Specifically, the FPU systems exhibited precisely the behavior to be expected of KAM nearly integrable systems. Chirikov then went further and presented theoretical evidence supporting the notion that, had FPU increased the strength of their nonlinear perturbations, they would have observed the onset of chaos. In retrospect, one notes that the Hénon–Heiles surfaces of section validate Chirikov’s predictions. Finally, Boris established that the resonance overlap criterion he applied to the FPU systems also applies to a much broader class of nonlinear systems. If Kruskal and Zabusky were the first to turn the FPU paradox into discovery, then Chirikov was assuredly the second, for he revealed that the KAM theorem is very nearly optimal. Indeed, it was violation of either conditions (ii) or (iii) of the KAM theorem that provided the first predictable route to chaos. The routes to chaos discovered later by Ruelle–Takens, May–Feigenbaum, and Pomeau–Manneville have been exhaustively discussed elsewhere [36]; thus, we here provide an elementary description of the route pioneered by Chirikov in his pursuit of an explanation for FPU. We do so in the full knowledge that Chirikov’s criterion is far from perfect; nonetheless, it remains the most widely used and provides the best order of magnitude estimate for the onset of chaos now available. We shall give an analytic expression for the Chirikov resonance overlap criterion after the following discussion.

We first seek to sketch a pictorially obvious explanation [37] of how a transition to chaos occurs when a nonlinear perturbation of H_0 becomes sufficiently large, i.e., when KAM’s condition (ii) is violated. For our H_0 , we take $H_0 = J_1 + J_2 - J_1^2 - 3J_1J_2 + J_2^2$, a two degrees of freedom system which is as convenient as it is arbitrary. Here each J_k is a momentum conjugate to an angle variable θ_k . Now the Hamiltonian $H_\alpha = H_0 + \alpha J_1J_2 \cos(2\theta_1 - 2\theta_2)$ is integrable, as is the Hamiltonian $H_\beta = H_0 + \beta J_1J_2^{3/2} \times \cos(2\theta_1 - 3\theta_2)$, due to the presence of constants $I_\alpha = J_1 + J_2$ and $I_\beta = 3J_1 + 2J_2$, respectively. The virtue of the integrable H_α and H_β is that their analytically computable surfaces of section each exhibit only one region of alternating elliptic–hyperbolic pairs, as can be seen in figs. 17 and 18. The two crescent-shaped, so-called 2–2 resonant zone in fig. 17 is due to the perturbation $\cos(2\theta_1 - 2\theta_2)$, which strongly distorts those H_0 tori having frequency ratios near 2/2. The 2–3 resonant zone seen in fig. 18 is a result of the $\cos(2\theta_1 - 3\theta_2)$ perturbation, which strongly distorts H_0 tori with frequency ratios near 2/3. Now as the size of these perturbations increase, their respective resonant zones grow wider and their centers move away from the origin. This opens the opportunity for these resonant zones to overlap before our very eyes.

In particular, from our knowledge of H_α , H_β , I_α , and I_β , we can determine the precise conditions under which edges of the independent 2–2 and 3–2 resonant zones first occupy the same position in phase space. Then, we let both the 2–2 and the 2–3 perturbations act on H_0 at the same time.

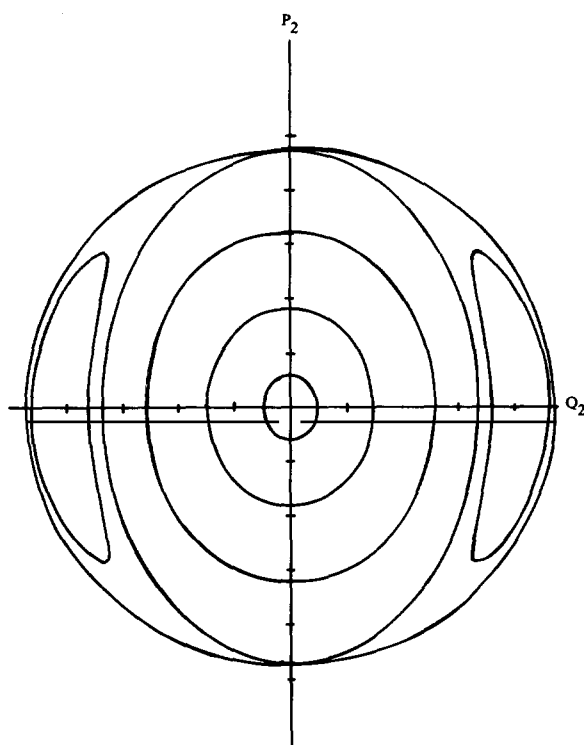


Fig. 17. A Poincaré section for the integrable Hamiltonian $H_\alpha = H_0 + \alpha J_1 J_2 \cos(2\theta_1 - 2\theta_2)$, where here and in the next two figures $H_0 = J_1 + J_2 - J_1^2 - J_1 J_2 + J_2^2$. Note that, as opposed to fig. 16, here only one set of elliptic–hyperbolic points appear, yielding a so-called chain of islands.

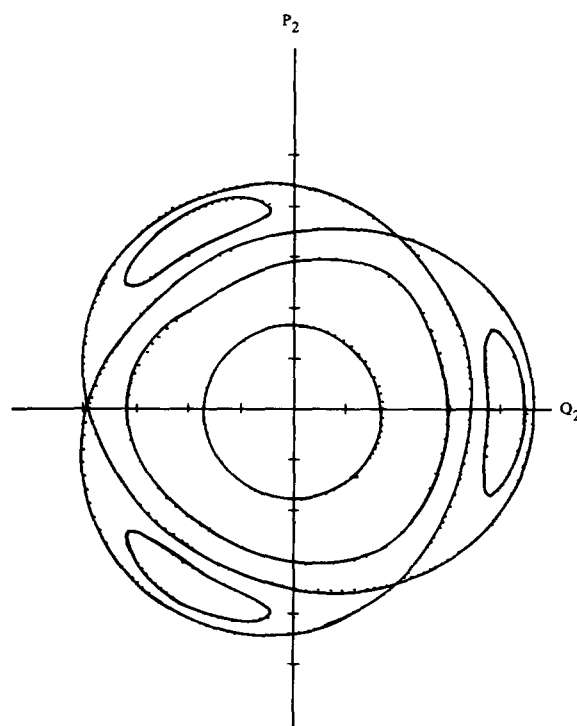


Fig. 18. Poincaré section for a distinct integrable Hamiltonian $H_\beta = H_0 + \beta J_1 J_2^{3/2} \cos(2\theta_1 - 3\theta_2)$. Here a single elliptic–hyperbolic set generates a single chain of three islands.

Specifically, we now regard

$$H_{\alpha\beta} = H_0 + \alpha J_1 J_2 \cos(2\theta_1 - 2\theta_2) + \beta J_1 J_2^{3/2} \cos(2\theta_1 - 3\theta_2)$$

as our full Hamiltonian. Mimicking Hénon–Heiles, we set $\alpha = \beta = 0.02$ and let the strength of the perturbation be determined solely by the energy. We now predict the onset of chaos in the full Hamiltonian to occur at $E \approx 0.2$ because this is the energy at which the computable crescent regions in figs. 17 and 18 first touch. Turning to the computer, in fig. 19a at $E = 0.056$, we see only the 2–2 resonance because the torus bearing the 3–2 frequency ratio has not yet appeared in the surface of section. However, in fig. 19b at energy $E = 0.18$, we see that both the 2–2 and the 2–3 crescent regions are present. Then in fig. 19c at $E = 0.2$, we note the surprise appearance of a 5–1 resonance between the 2–2 and 2–3; but in fig. 19d, we observe a small emerging region of chaos as predicted by the integrable approximations. Although the chaos of fig. 19d is drawn separately, it actually surrounds the larger crescents in fig. 19c. Finally, fig. 19e at energy $E = 0.2095$ reminds us of the band of chaos appearing in Hénon–Heiles’ fig. 12. This then briefly illustrates the first KAM/Chirikov route to chaos.

Returning briefly to Chirikov’s resonance overlap criterion, Boris first normalizes a system’s relevant

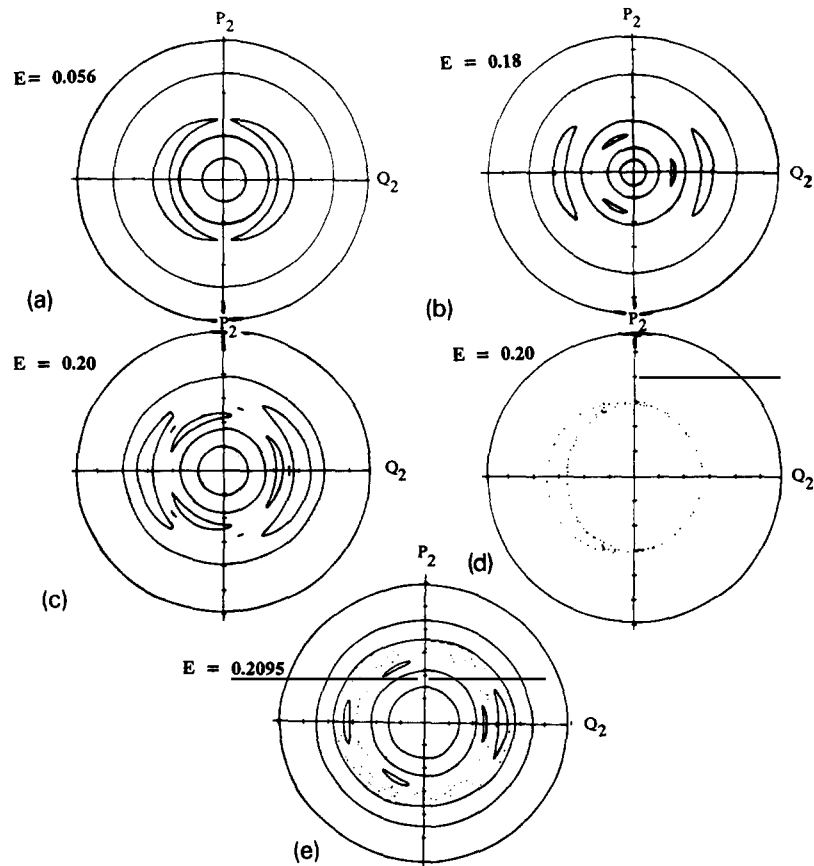


Fig. 19. Five surfaces of section showing the effect of adding the perturbations of both H_α and H_β to H_0 and then increasing the strength of these perturbations. Specifically, we set $\alpha = \beta = 0.02$ and then increase the energy as a single perturbation parameter. In (a) at $E = 0.056$, only the H_α island chain can be seen. However, in (b), at $E = 0.18$, both the H_α and H_β island chains have appeared though they are well separated. In (c) and (d), both at energy $E = 0.20$, we note the sudden appearance of a higher-order island chain and a very small erratic region of chaos. For clarity, (c) and (d) have been drawn separately; imagine them superposed. Finally at $E = 0.2095$ in (e), we see a band of chaos reminiscent of that seen in the Hénon–Heiles problem. The central point of these figures is that chaos occurs when the integrable island chains (resonances) overlap.

phase space volume to unity. He then estimates the volume V_R of all resonant zones (as in figs. 17 and 18) as if each interaction term in the potential acted alone. He then asserts that widespread chaos occurs when $V_R \approx 1$.

Let us now turn to systems which lead to violation of the KAM frequency condition (iii). In order to violate the KAM frequency condition in the strongest possible way, we elect [38] to consider an H_0 having constant frequencies. Here, $H = H_0 + \gamma H_1$, where

$$H_0 = J_1 + 2J_2 + 3J_3, \quad H_1 = [\alpha J_1 J_2^{1/2} \cos(2\theta_1 - \theta_2) + \beta (J_1 J_2 J_3)^{1/2} \cos(\theta_1 + \theta_2 - \theta_3)].$$

As before, J_k is the momentum canonically conjugate to position variable θ_k . Recalling that $\omega_k \equiv \partial H_0 / \partial J_k$, we note that $\omega_1 = \omega_2/2 = \omega_3/3$ independent of the J_k or θ_k . The upshot is that all H_0 tori bear rational frequencies in the ratio 1/2/3. Thus, the resonant 2–1 perturbation $\cos(2\theta_1 - \theta_2)$ and the resonant 1/1/1 term $\cos(\theta_1 + \theta_2 - \theta_3)$ overlap throughout phase space. In addition, if we introduce the

canonical transformation $J_k = \mathcal{I}_k$, $\theta_k = \psi_k + kt$, $k = 1, 2, 3$, then we obtain

$$\mathcal{H} = \gamma[\alpha \mathcal{I}_1 \mathcal{I}_2^{1/2} \cos(2\psi_1 - \psi_2) + \beta(\mathcal{I}_1 \mathcal{I}_2 \mathcal{I}_3)^{1/2} \cos(\psi_1 + \psi_2 - \psi_3)]$$

as the transformed Hamiltonian. The form taken by \mathcal{H} now exposes a remarkable fact, for, if we now scale the time according to $t = \gamma\tau$, we find

$$\hat{\mathcal{H}} = [\alpha \mathcal{I}_1 \mathcal{I}_2^{1/2} \cos(2\psi_1 - \psi_2) + \beta(\mathcal{I}_1 \mathcal{I}_2 \mathcal{I}_3)^{1/2} \cos(\psi_1 + \psi_2 - \psi_3)],$$

from which γ has completely disappeared! Thus, despite the fact that γ appears as a parameter measuring perturbation strength in $H = H_0 + \gamma H_1$, in fact it merely scales the time. Whatever the character of the motion for H , whether integrable or chaotic, varying γ changes only the rate at which things happen, not what happens. Moreover, this remains true no matter how small the value of $\gamma > 0$. Second, the form of $\hat{\mathcal{H}}$ (or \mathcal{H}) makes it clear that $\mathcal{I} = \mathcal{I}_1 + 2\mathcal{I}_2 + 3\mathcal{I}_3$ is a constant of the motion (obviously, so is $I = J_1 + 2J_2 + 3J_3$). Invoking techniques well known to students of advanced classical dynamics [39], this constant can be used to reduce the number of degrees of freedom for this system from three to two, thereby permitting use of two-dimensional, plane surfaces of section. We here omit analytical details and proceed straight to the numerical results shown in fig. 20a, b. Figure 20a reveals a typical surface of section for the case in which phase space exhibits a regular and a chaotic component; fig. 20b presents a typical surface of section for which most of phase space is covered with chaotic trajectories. These two figures indicate the change in surface of section which can occur when system parameters are varied; for details see ref. [38].

The quite remarkable feature of these surfaces of section is that they are invariant under changes in the value of γ for any $\gamma > 0$. Thus, there is a discontinuous change from the integrable motion of H_0 to the chaotic motion of the full H the moment γ increases away from zero. Although such behavior is common in billiard systems, the results described here reveal that it also occurs in systems having smooth potentials. In fact, this behavior is quite common in smooth systems. The only requirements for

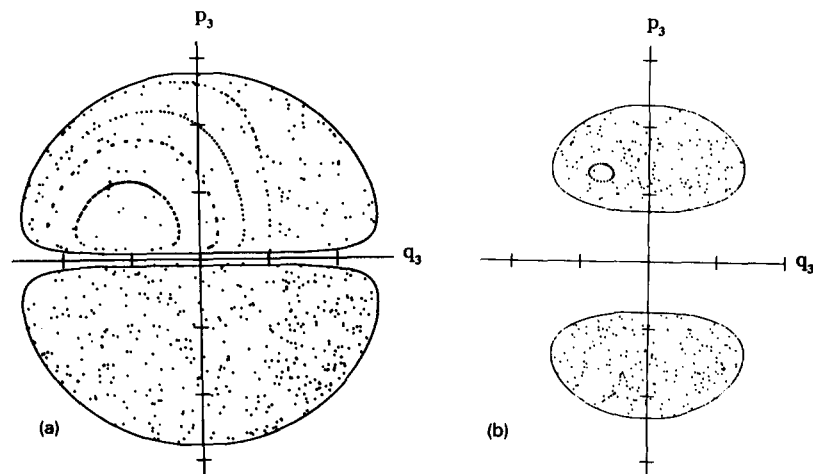


Fig. 20. (a) Both order and chaos in the surface of section for the Lunsford–Ford [38] Hamiltonian. This surface of section is invariant as the nonlinearity parameter γ tends to zero. (b) Chaos dominates; this surface of section too is invariant as γ tends to zero. These figures show the effect of varying a system parameter; for details see ref. [38].

this behavior in Hamiltonian systems expandable about a stable equilibrium point or periodic orbit are that the constant frequencies of the quadratic terms exhibit sufficient rational dependences that the cubic couplings can resonantly couple all degrees of freedom before quartic or higher-order terms can add nonlinear corrections to the constant harmonic frequencies.

For illustrative purposes, these conditions were forced upon the simple, three degrees of freedom Hamiltonian system $H_{\alpha\beta}$ considered above; however, in many-body systems, their satisfaction is both frequent and automatic. Two immediate consequences accrue. First, chaos is now seen to be ubiquitous in the macroscopic world. But second and equally important, this second KAM/Chirikov route to chaos is also a route to classical statistical mechanics which has for decades held the belief that its justification would eventually derive from classical mechanics itself. Consider, for example, equilibrium statistical mechanics, which computes equilibrium quantities from the partition function $Z = \int dq dp e^{-\beta H_0}$ on the assumption that the weak γH_1 which brings the system to equilibrium need not be added to the H_0 in Z . KAM/Chirikov now permit an a priori proof of this assumption to replace the earlier a posteriori arguments touting that “it works”.

In concluding this section, let us note that violation of KAM condition (ii) provides a route to chaos with a threshold just as do several other paths to chaos. However, violation of KAM condition (iii) yields a discontinuous jump to chaos from the unperturbed integrable system. Both routes have relevance to many areas of physics including statistical physics.

We now present an example from nonequilibrium statistical mechanics which carries us full circle back to FPU. Specifically, we substantiate their belief that a computer can provide an illuminating first principles verification of thermal diffusion in the dynamics of a nonlinear Hamiltonian system, i.e., a derivation containing no phenomenological assumptions.

5. The ding-a-ling model

“It seems there is no problem in modern physics for which there are on record as many false starts, and as many theories which overlook some essential feature, as in the problem of the thermal conductivity of nonconducting crystals.”

R.E. Peierls [40]

What is the nature of the problem Peierls highlights? First, recall that energy (heat) transport in an insulating solid is governed by the phenomenological Fourier heat equation [41] $J = -K\nabla T$, where J is energy (heat) current, ∇ is the gradient operator, T is temperature, and K is a size independent, intrinsic system property called the thermal conductivity. This then is the problem. There is no first principles, analytic derivation of this phenomenological law nor, prior to KAM/Chirikov, were there valid criteria defining a category of systems whose numerical integration might be expected to yield a proper thermal conductivity, not even when attention is restricted solely to lattice energy transport. Zabusky suggests that this lack was one of the prime forces driving FPU to study one-dimensional nonlinear lattices. At first blush, it might appear that the FPU calculations unveiled yet another “false start”; however, the FPU preprint described not a failure, but a paradox demanding resolution. Specifically, the FPU results challenged the theoretical community to explain why the well-known theorems of Poincaré, Fermi, and Siegel did not, in fact, define the proper criteria for observing a normal thermal conductivity. Although there is still no first principles analytical derivation of the

Fourier heat law, direct numerical integration of Newton's equations has verified that chaotic dynamical systems do in fact exhibit an energy transport governed by the Fourier heat law. Indeed, the key ingredient is now known to be chaos [42]; however, before presenting the evidence supporting this conclusion, let us stroll along part of the path which led to it. Following FPU, we confine our attention to one-dimensional nonlinear systems. They clearly offer greater ease of numerical integration, but more important they can, folklore to the contrary notwithstanding, exhibit an energy transport which obeys the Fourier heat law.

For a one-dimensional lattice system at equilibrium, the average energy flow at any point is zero. Nonetheless, there are fluctuations in which the net energy flow reverses its direction in a highly erratic and seemingly unpredictable fashion. If a temperature difference is placed across the ends of such a lattice system, energy fluctuations are expected to continue almost as before, only now the temperature difference slightly favors fluctuations in one direction over the other. Energy transport is thus seen to resemble a random walk in which on average there is no net movement but in which root mean square deviation can nonetheless grow. More than a mere analogy is involved here. Indeed, Wang and Uhlenbeck [43] announced many years ago that the heat equation is the continuum limit of a discrete random walk. But if we now wish to establish that a deterministic Newtonian system exhibits energy transport obeying the Fourier heat law, we find ourselves facing not merely that FPU paradox but the much deeper paradox involving how a predictable, deterministic system can ever exhibit unpredictable, random behavior.

Clearly nothing in the traditional background of most physicists prepares them for such contradictions; but worse, even the traditional definition of classical chaos involving sensitive dependence, Liapunov numbers, and the like, leaves the scientific audience equally unprepared. Indeed, one finds even the most recent issues of journals such as *Physical Review Letters*, *Physica D*, or *Nature*, littered with terminology such as “seemingly random”, “apparently unpredictable”, or “deterministic chaos”.

Fortunately, the need for such dissembling has long since passed. For systems chaotic in the sense of positive Liapunov number are also deterministically random in the sense [44] of algorithmic complexity theory – see appendix A for details. At this point let us merely state that the paradox can be resolved merely by noting that nothing in principle prevents a deterministic orbit from being a realization of a random process. In any event, if one wishes to expose a classical system yielding diffusive energy transport then one is forced to regard deterministic randomness (chaos) as a necessary ingredient. But is it also sufficient?

Once Casati and Ford [45] established that the unequal-mass Toda lattice, unlike its integrable equal-mass brother, exhibits a transition to chaos with increasing energy, they immediately recognized that this unequal-mass system was a prime candidate for demonstrating the validity of the Fourier heat law via direct numerical integration of its equations of motion. However, at the time they were enmeshed in a numerical investigation of energy transport in the 1-D, unequal-mass hard-point gas, which, as particle number increased, appeared to be always teetering on the brink of yielding a thermal conductivity independent of length. In the equal-mass hard-point gas, as in the equal-mass Toda lattice, energy is transported by unattenuated solitons. For both, heat current is proportional to temperature difference rather than gradient, and conductivity K is therefore proportional to system length. With the introduction of distributed mass impurities, the solitons are attenuated permitting the hard-point gas to become mixing (but not chaotic) and the Toda lattice to exhibit a transition to chaos. This being the case, why did Casati et al. not immediately drop the hard-point gas and turn to the Toda lattice? To understand this point, one must recall that initially close orbits for mixing systems are rigorously known to separate according to some polynomial function of the time t whereas initially close chaotic orbits

separate exponentially with the time. However, if the polynomial function of t is of sufficiently higher order, then only extreme care and great numerical accuracy could distinguish mixing from chaos, to distinguish very weak length dependence from no length independence in K .

Despite many hours of computer time, reams of computer paper, countless mass distributions, and particle number increased to our limit, soliton-like entities continued to move through our unequal-mass, hard-point gas systems carrying energy proportional to temperature difference rather than gradient. Moreover, as we varied the mass distributions and increased system particle number, the conductivity would tend toward but never reach a constant value. Surveying the character of our evidence, we concluded that mixing, at least in the hard-point gas, is not rapid enough to yield a length-independent thermal conductivity. We thus turned to an all-out assault on the unequal-mass Toda lattice, but alas, the seemingly indomitable “soliton” again defeated our best efforts. Stacks of computer output for the Toda lattice led us to believe that, could we have gone beyond our 200 particle limit, a fully diffusive energy transport might have been obtained. Indeed for some mass distributions, our results were tantalizingly close, but they never stabilized. We roundly cursed the day the soliton was born; we haunted the halls of soliton conferences in hopes of finding its Achilles heel. And then, Glory Hallelujah, young Billy Visscher introduced us (for details, see ref. [41]) to the ding-a-ling model shown in fig. 21.

Figure 21 exposes a one-dimensional, equal-mass system composed of free particles alternating with harmonically bound ones. Despite its hybrid character, Visscher had high hopes for this model. First, it was computationally tractable, but even more important, the rapid oscillations of the bound particles would lead to effectively random phases in sequential collisions with the free particles. If system motion could thereby exhibit enough randomness, then diffusive energy transport would appear likely. Casati et al. saw three additional virtues in the model. First, suppose all particles in fig. 21 are at rest; then let the leftmost free particle be given a “hammer-blow” creating a “soliton” moving to the right. After being struck by this free particle, the first bound particle will move to the right; however, if the restoring force on this bound particle is large enough, it will not swing out far enough to hit the neighboring free particle to the right. Thus, the soliton dies after just one collision! Nonetheless, and this is the second point, if the amplitude of the initial soliton-type sound pulse is sufficiently large, then it can propagate through to the other end of the system despite being strongly attenuated en route. And third, the final state for this system can be exquisitely sensitive to a slight change in initial state, not because of isolated binary collisions between free and bound particles, but because a free particle can have multiple collisions with a given bound particle before colliding with its other bound neighbor. It is these multiple collisions which yield the chaos, the deterministic randomness, shown in fig. 22.

Figure 22a pictures the simplest version of our system, which places one bound and one free particle on a ring (periodic boundary conditions). For this simplest system, we may construct the surfaces of section shown in figs. 22b, c. Once particle number N is fixed, then all other parameters for this system can be “scaled” out save one which we chose to be ω , the angular frequency of the bound particle. We

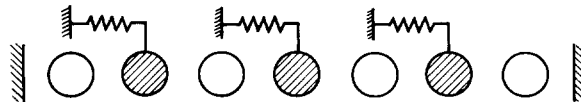


Fig. 21. This figure reveals the ding-a-ling model (due to Bill Visscher) to be a one-dimensional system composed of free particles alternating with harmonically bound particles. The model is quite nonphysical yet nonetheless retains that essential feature required to exhibit a thermal conductivity independent of length.

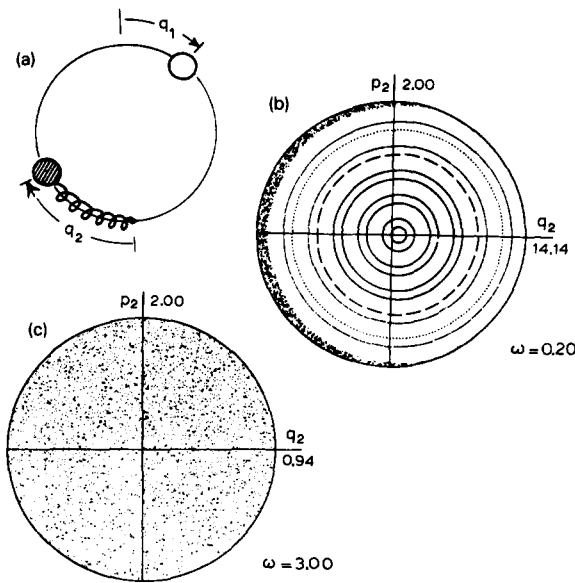


Fig. 22. (a) The simplest ding-a-ling model having two particles – one bound one free – moving on a ring. (b) A surface of section for this ding-a-ling model when the spring is sufficiently weak that the motion is close to that of the integrable hard-point gas. (c) For sufficiently stiff spring, one obtains a chaotic surface of section.

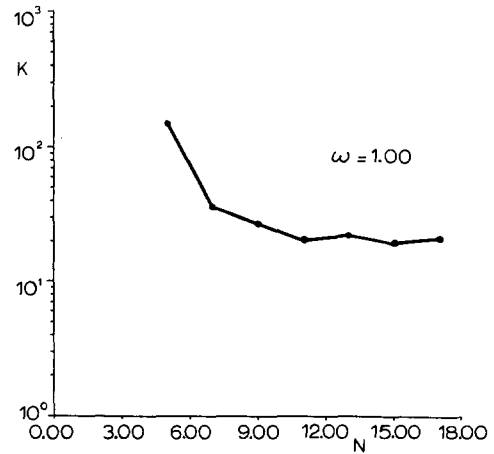


Fig. 23. This figure plots the thermal conductivity for the ding-a-ling model as a function of particle number. Here hot and cold reservoirs are placed at the left and right ends of the system, respectively. The conductivity K is computed from $J = -K\nabla T$ and it becomes independent of length at about $N = 10$.

may also view ω as specifying the stiffness of the harmonic spring. When $\omega = 0$, this system becomes the two-particle hard-point gas, which is integrable. Figure 22b shows the nearly integrable, weak-spring surface of section at $\omega = 0.20$. Here, smooth curves exist almost everywhere except for the thin region of chaos at the extreme left of the figure, where multiple collisions are occurring. Chaos becomes widespread at $\omega = 1.00$ (not shown), and in fig. 22c the transition to total chaos at $\omega = 3.00$ appears complete. For systems with particle number greater than two, we have verified their transition to total chaos via exponential orbit separation and Liapunov numbers. With increasing N , the value of ω at which chaos becomes widespread rapidly decreases.

We now placed the system shown in fig. 21 between two simulated heat reservoirs and numerically integrated the equations of motion using $\omega = 1$. Next, we established that the heat current J and the temperature gradient ∇T achieved a constant steady state value. We then computed the thermal conductivity from the heat equation $J = -K\nabla T$, where $\nabla T = dT/dx$ for these one-dimensional systems and where particle temperature T is taken to be twice the particle’s kinetic energy. Finally, we computed K over a range of particle number N and verified, as shown in fig. 23, that K becomes size independent for $N \geq 10$. Finally, our reservoir value for K was corroborated via two independent calculations: the Green–Kubo formalism and a random phase argument – details are given elsewhere [41].

It is now time to discuss why we named our system the ding-a-ling model. Its first meaning derives from a Bill Visscher phantasy in which each free particle is viewed as a clapper swinging ‘twixt neighboring oscillators and forcing them to ring out like bells. But quite aside from lending itself to suggestive onomatopoeia, there is a second reason for the name. Webster’s dictionary states that ding-a-ling is most likely a euphemism for damn fool, and ours is a damn fool model indeed. This

hybrid, this unphysical half-breed of questionable ancestry – half ideal gas, half harmonic oscillator – is a true ding-a-ling for certain. Readers are therefore to be forgiven if their first reaction to the diffusive energy transport exhibited by the ding-a-ling model is to regard it as a freak occurrence in an absurd model. But au contraire, quite the opposite is true.

Had we wished merely to predict a lattice thermal conductivity for some laboratory substance starting from Newton’s equations, we could have positioned a three-dimensional, many-body system having a physically realistic interatomic potential between simulated thermal reservoirs and then let a computer churn out an answer to be compared with experiment. There is much to be learned from such calculations as the excellent paper by McDonald and Tsai reveals [46]. However, the ding-a-ling model serves a quite different purpose. It proves that a dramatically short, one-dimensional lattice system can exhibit diffusive energy transport provided it has that one ingredient essential for the task. With the single-minded intent of exposing that essential ingredient, the ding-a-ling model has abstracted away all the seemingly crucial attributes of a proper physical system save the one unique attribute required to yield a diffusive energy transport. Like the Cheshire cat in *Alice in Wonderland*, in the ding-a-ling model everything has disappeared except the smile. In this regard, we must emphasize that attenuation of solitons is a problem only for small systems. For large (laboratory-sized) systems, the transition of energy transport as pure sound to heat is concurrent with the transition from order to chaos. In summary, deterministic randomness (chaos) is the sine qua non for a proper thermal conductivity.

This section has emphasized the contribution of the ding-a-ling model to the problem of lattice thermal conductivity because it is a direct descendant of the FPU problem. Obviously, many others have sought to expose the essentials needed for diffusive energy transport and the motivation for the ding-a-ling model owes much to the efforts of others. Work on harmonic systems with impurities has been reviewed by Visscher [47] and by Jackson [48], who also reviews the research on nonlinear systems. But especially relevant to the present discussion are the papers of Mokross and Büttner [49] and those of Jackson and Mistriotis, [50], for both these papers investigated energy transport in diatomic Toda lattices. Mokross and Büttner investigated diatomic Toda lattices for particle number up to $N \approx 30$ and reported they had obtained a proper, size-independent thermal conductivity. Jackson and Mistriotis, on the other hand, asserted that they could obtain a size-independent conductivity only for $N \geq 250$. The unpublished results of Casati et al. support this Jackson–Mistriotis conclusion. Indeed, there is much overlap in the conclusions reached by Jackson–Mistriotis and Casati et al. Details may be found in their respective papers.

6. Discussion

The FPU paradox forces us to face some of our deepest insecurities. Given the Hamiltonian for a system, what is the character of its motion? What requirements must be imposed on a dynamical system in order that an approach to equilibrium be guaranteed and that this approach proceed at the proper rate? Can statistical mechanics – both equilibrium and nonequilibrium – be derived from the underlying dynamics? And now the questions bifurcate, evolving into questions which probe almost every area of science. Dyson’s quite pertinent comment, “Ford’s explanation cannot be regarded as complete”, lingers, for it applies not just to Ford but to all. Indeed, the “full and final” explanation of FPU still pends. It is this very fact which makes the FPU paradox such a delightful pedagogical “skeleton” upon which to drape the evolving story of nonlinear dynamics/chaos. This review is but another retelling of

that story by one intimately involved in its unfolding. It is based on a lecture first prepared for a Los Alamos audience but subsequently presented elsewhere. It has now reached the graduate student level as the opening lecture in an advanced graduate course in nonlinear dynamics/chaos. This review represents its first appearance in print, but it may appear later as the opening chapter in a graduate text. A good conference talk never dies, it simply metamorphoses over . . . and over . . . and over again.

The FPU paradox was not only instrumental in the development of solitons, heavy breathers, inverse scattering, completely integrable systems, and the like but also in the development of Chirikov's resonance overlap criterion for the onset of chaos. But in addition, FPU is a close cousin to the surprise packages contained in the Hénon–Heiles system and the Toda lattice, which latter links back to solitons, breathers, etc. Finally, its resolution led to the understanding that few-body systems can behave just as randomly as do many-body systems; indeed, it is now appreciated that statistical behavior in many-body systems is not so much a consequence of the law of large numbers as of the ubiquity of chaos. The marriage of classical mechanics and classical statistical mechanics is now only a matter of time, although the final prenuptial agreement may not be signed within our lifetime.

Statistical mechanics frequently insists on the thermodynamic limit in which system volume and particle number tend to infinity whereas classical dynamics still has not fully mapped out the domains of behavior in finite systems. In an effort to bridge the perceived gap between dynamics and statistical mechanics, a growing number of investigators [51] have sought, with mixed results, to establish that chaos occurs at vanishingly small nonlinearity as particle number tends to infinity. These computer studies form a valiant first attack on a problem whose subtle intricacies dwarf those of the KAM theorem by orders of magnitude. What are these intricacies? We have space to list only a few. First, the thermodynamic limit is, strictly speaking, only a mathematical convenience, not a physical necessity. Three independent groups have, for example, established [42, 49, 50] that small, even one-dimensional systems can exhibit a normal, Fourier conductivity provided phase space is dominated by chaos. Similarly, Chirikov's kicked rotor, though sufficiently chaotic at large nonlinearity to exhibit diffusion, retains small islands of stability no matter how strong the nonlinearity [52]. In other systems, chaos dominates no matter how small the nonlinearity^{*)}; in yet others the amount of chaos at first increases and then decreases with increasing nonlinearity.^{**)} Such variety makes generalities suspect.

But what now of the subtleties? Return to Siegel's theorem [13] regarding analytic Hamiltonians which can be expanded in a power series about their equilibrium points. Since nonintegrable systems are dense in their $\{c_k\}$ -space, integrable systems can in general be distinguished from their dense nonintegrable neighbors only if all coefficients in their power series are known to infinite precision. Physicists do not often enjoy this luxury. As a final subtlety, Moser [13] points out that, if the definition of neighborhood in $\{c_k\}$ -space be slightly altered from the intuitively obvious definition Siegel uses, then integrable systems are also dense in $\{c_k\}$ -space! We thus reach the distressing conclusion that distinguishing integrable from nonintegrable systems is in general no easier than distinguishing rational from irrational numbers.

Placed in perspective, all these problems reveal finite human beings using finite tools to reach for infinity – the infinitely large, the infinitely small, the infinitely complex. Truly, what fools we mortals be; we fail to listen even to our own prophets! Avagadro counted the particles in a box and found them

^{*)} In addition to the example presented in ref. [37], the 3D hard-point gas is integrable, but when the points become spheres, system motion is chaotic no matter how small the radius $r > 0$ of the spheres.

^{**)} Consider the one-dimensional Lennard-Jones gas. At low energies, its motion is negligibly different from that of coupled harmonic oscillators. As its energy is increased, a transition to chaotic behavior occurs. But at extremely large energy, the amount of chaotic behavior must decrease rapidly as system motion tends towards that of the integrable 1D hard-point gas.

to be finite. Einstein patiently explained to all that man's ultimate speed is finite. Heisenberg pointed out that man's ability to measure conjugate variables is finite. Gödel established that man's ability to provide a complete mathematical description of his universe is finite – see the appendix below. But still we do not listen. The overwhelming majority of chaos theorists valiantly cling to the notion of deterministic predictability and speak of “deterministic chaos”. By this, they mean that their most accurate available knowledge of an initial state permits them to “predict” future states with exponentially decreasing accuracy. But algorithmic complexity theory – again consult the appendix – establishes that this is precisely the type of “prediction” one could provide for a random walk. And in fact, a chaotic process is random. It is also deterministic in the sense that the governing equations satisfy the conditions of some existence–uniqueness theorem. Thus, some few have begun to refer to chaos as “deterministic randomness”. In the context of this paragraph, this term makes it clear that we cannot obtain any more information about the future of a chaotic state sequence than we put in at the onset, and the amount we put in is always finite. In consequence, another fundamental limitation on man lies exposed. Chaos is thus opening a new era in science. This entire review has pointed toward this final conclusion. However, as readers consider whether to accept or reject our conclusion, they might wish to contemplate the following observation:

“I know that most men, including those at ease with problems of the greatest complexity, can seldom accept even the simplest and most obvious truth if it be such as would oblige them to admit the falsity of conclusions which they reached perhaps with great difficulty, conclusions which they have delighted in explaining to colleagues, which they have proudly taught to others, and which they have woven, thread by thread, into the fabric of their lives.”

Leo Tolstoy

Acknowledgement

Were I to list that legion of colleagues whose kind words and helpful hints guided a once untutored Georgia boy over the jargon-laden backroads of nonlinear dynamics/chaos, not even those listed would read to the end. Thus, I here spare both reader and printer by simply offering my deepest and most heartfelt thanks to all those not listed here. But my gratitude also extends to each new generation of students who view history through a telescope's far end and are therefore ever appreciative of knowledge that nonlinear dynamics did not begin with Feigenbaum or even Lorenz. It is they who will implement what we ancients dream but dare not believe. They are the reason for this article.

Appendix A. Algorithmic complexity theory

The lexicographer [53] surveys human usage and publishes the consensus – **chaos**: a state of things in which chance is supreme. The chaologist [36] surveys his discipline and announces definitional anarchy, even though greater resolution might have revealed but one definition having a thousand names. In the current literature, one finds “erratic”, “irregular”, “disordered”, “seemingly unpredictable”, “apparently random”. Greater technical sophistication invokes positive Liapunov numbers, positive metric or topological entropy, everywhere negative curvature, or the like. Were the dynamical systems under

scrutiny not labeled deterministic, all the above defining terms would naturally fall under the obvious rubric, “random”. But this word immediately implies the term “deterministic randomness”, which a physicist instinctively feels is equivalent to the oxymoron “predictable unpredictability”. But the existence–uniqueness underpinning our Laplacian clockwork universe notwithstanding, determinism and predictability are not synonyms. Indeed, there is life beyond the conventional “deterministic chaos”; however, we must develop a new definition of randomness in order to find it. To that end, we now present the rudiments of algorithmic complexity theory, also known as algorithmic information theory.

At the foundation of algorithmic complexity theory lies the notion of randomness in finite and infinite digit strings. To give meaning to randomness, complexity theory introduces a quantity K_N , called complexity, defined as the bit length of the shortest algorithm (computer program) capable of computing a given sequence of N bits.

One immediately wonders if complexity can be made machine independent. In answer, Kolmogorov has proven the existence of a universal machine U such that $K_U(x) \leq K_{\mathcal{A}}(x) + C_{\mathcal{A}}$, where U denotes universal and \mathcal{A} denotes arbitrary machine, where x denotes the finite output binary string, and where $C_{\mathcal{A}}$ depends on \mathcal{A} but not x .

Next, a reader might inquire if complexity K_N can always be precisely determined? To answer, recall that, if K_N is the complexity of a given N -bit sequence, then no $(K_N - 1)$ bit program can compute this sequence. Suppose then we seek to verify someone’s assertion that a specified sequence has complexity K_N by sequentially running all programs having $(K_N - 1)$ bits. Many of these programs will at best output some nonsense result and halt, but some of them may run without halting for a time longer than we have to wait. How then can we be certain that at least one of these latter programs will not eventually print out the specified sequence, revealing that its actual complexity is $(K_N - 1)$ or less? The answer to this question lies at the bedrock foundations of mathematics, for Turing’s Halting Theorem [54], the computing man’s version of Gödel’s theorem, asserts that the only way to know whether an arbitrary computer program will accomplish its task and halt is to let it run and see. Determining a precise value for complexity K_N thus lies beyond human capability. Nonetheless, K_N can and does serve as a useful mathematical construct, but of greater significance for us, K_N can in most cases be estimated as well as is needed.

To illustrate, let us now estimate complexity for some informative examples. For simplicity, we shall assume all sequences to be binary; were the original sequence given in some other base, we could easily convert it to binary via a subroutine whose fixed bit length will not materially affect K_N , provided N is large relative to the bit length of the subroutine. Indeed, the following estimates become useful only when N is sufficiently large that the bound on K_N is dominated by N .

First, note that all N -bit binary sequences can be printed by the copy program, “PRINT $[b_1, b_2, \dots, b_n]$ ”, where $[b_1, b_2, \dots, b_n]$ denotes any arbitrary sequence. Then consider long sequences so patternless they cannot be computed by any algorithm appreciably shorter than the copy program. Clearly, an upper bound on the complexity of such sequences is given by $K_N \leq N + C_1$, where $C_1 \ll N$ is a constant which accounts for the bit length of the computer operating system, internal functions, and the like; a lower bound on the complexity of such sequences reads $K_N \geq N - C_2$, where $C_2 \ll N$ sets our cutoff for patternless sequences. Turning now to the opposite extreme of ordered sequences such as a string of N ones. This sequence can be computed by a program, “PRINT ONE, N TIMES”, whose bit length is almost completely exhausted by the $\log_2 N$ bits required to specify the integer N . For this highly ordered sequence, an upper bound on complexity may be written $K_N \leq \log_2 N + C_3$.

Clearly all these bounds require that N be sufficiently large that N or $\log_2 N$ dominate their associated C 's. However, “sufficiently large” must not be thought to imply that our inequalities become accurate only in the limit as $N \rightarrow \infty$; this phrase is here used solely to ensure that K_N reflect a property of the sequence rather than the computer. To fully appreciate this point, rewrite the last two inequalities as $K_N \geq N[1 - (C_2/N)]$ and $K_N \leq \log_2 N[1 + (C_3/\log_2 N)]$. It is now clear that (C_2/N) and $(C_3/\log_2 N)$ represent the fractional error made in writing the more useful estimates $K_N \approx N$ and $K_N \approx \log_2 N$. How “sufficiently large” N must be is determined by the error permitted in the physical or mathematical application being considered. However, it must be emphasized that estimates of complexity become meaningless when applied to sequences so short that N or $\log_2 N$ is less than their relevant C 's.

Following Kolmogorov, Chaitin, and Solomonov (see ref. [55]), we now assert that an N -bit sequence is random provided that its complexity K_N is approximately equal to N . Random sequences are informationally incompressible, so unpredictably erratic that they cannot be computed by any algorithm whose bit length is appreciably less than that of the sequence. Moreover, as Martin-Löf has shown [44], such sequences are nothing less than realizations of conventionally defined stochastic processes. But now to ensure that the necessary phrase, “approximately equal to”, can be made sufficiently precise that the definition of algorithmic randomness is seen to be valid when the value of N is large, let us introduce Martin-Löf's theorem [44]: The fractional number F of N -bit binary sequences having complexity $K_N \geq N[1 - (C/N)]$ satisfies $F \geq (1 - 2^{-C})$, where C is a positive integer in the range $0 < C < N$. This theorem permits us to choose C such that F is as close to unity as we please; we can then choose N such that K_N approaches N as close as we please. Thus, when $N \gg C \gg 1$, we have that the overwhelming majority of the corresponding N -bit binary sequences are unequivocally random, i.e., $K_N \approx N$. To put meat on the bare bones of these arguments, consider the specific case in which $C = 5$ and $N = 100$. Then more than 96% of the 2^{100} ($\approx 10^{30}$) 100-bit sequences have complexity $K_{100} \geq 95$. Truly, among N -bit sequences randomness reigns.

But in the remaining small set of sequences for which $K_N \neq N$, there is a subset of informationally compressible sequences having $K_N \ll N$. Kolmogorov, Chaitin, and Solomonov call such sequences nonrandom. Among these, there is a subset whose information content is logarithmically compressible, i.e., $K_N \leq \log_2 N + C$, for all N such that $\log_2 N \gg C$; it is precisely these highly ordered sequences which occur most frequently in applications. Note that, because of their logarithmic compressibility, these sequences are just as unequivocally nonrandom as the $K_N \approx N$ sequences are unequivocally random. Moreover, since N -bit sequences divide into that vast majority which are random and that small minority whose information content is logarithmically compressible, only a small subset indeed remains to occupy that narrow and unimportant (to us) border where randomness blends into nonrandomness. The meaning of complexity is now well defined for finite sequences, but how are we to extend the definition to infinite sequences?

Kolmogorov originally proposed that an infinite sequence should be considered random if all its finite subsequences of length N had complexity $K_N \approx N$. However for increasing N , Martin-Löf demonstrated that the complexity of finite sequences oscillated in an irregular way between $K_N \approx N$ and $K_N \approx N - \log_2 N$. The problem is that even random sequences sometimes have quite extended nonrandom segments. Various ways have been suggested to circumvent this problem and each has its advocates. Here we elect to follow Alekseev and define the complexity K_∞ of an infinite sequence via the equation $K_\infty = \lim_{N \rightarrow \infty} (K_N/N)$. With this definition in hand, we again follow Alekseev and colleagues and assert that an infinite sequence is random when $K_\infty > 0$ and nonrandom when $K_\infty = 0$. It is thus common to speak of positive or null complexity as a substitute for saying random or nonrandom. These definitions have the virtue of eliminating the oscillations in K_N and of providing a sharp divide between random and nonrandom. In addition, using these definitions, Martin-Löf has proven that sequences having

positive complexity are realizations of a random processes which pass all humanly computable tests for randomness; this proof provides the iron-clad link between conventional definitions and the algorithmic definition of randomness.

We can now at last forge the connection [56] between the conventional definitions of chaos and its definition as deterministic randomness. The intuitive definitions “erratic”, “irregular”, “disordered”, “seemingly unpredictable”, “apparently random” can be subsumed under the slightly more technical “exponential sensitivity of final state upon initial state’. In mathematical jargon, exponential sensitivity means positive Liapunov numbers. But now let us inquire why this most commonly accepted definition [57] focuses its attention so intently upon exponential growth of initial error in the time evolution of chaotic dynamical systems? Why can it not be satisfied with an error which grows according to a power law having a large exponent, or why not the opposite where error grows like an exponential raised to an exponential?

The answer is revealing. Simple exponential error growth (*in systems with bounded state space, of course*) is precisely the point at which our calculations lose about one digit of accuracy per suitably chosen unit of time. Thus, if we wish to maintain constant calculational accuracy over an extended interval, we must input about as much information as we get out of our calculations. This is the point at which our IBM or CRAY computers begin, in effect, to execute the copy program discussed earlier; indeed, they become elaborate Xerox machines. In summary, it is the point at which our deterministic algorithms are in the process of computing orbits which are both deterministic and algorithmically random. There is no contradiction here, since the existence and uniqueness (determinism) of chaotic orbits does not preclude them from being realizations of some random process. Consequently, it now becomes clear that the definition of chaos as exponential sensitivity or positive Liapunov numbers is fully equivalent to its definition as deterministic randomness; which definition one uses is a matter of choice.

The above discussion has been at the intuitive level; mathematical rigor has been supplied by Alekseev, Yakobson, and Brudno (see ref. [58]). In closing, let us observe that algorithmic complexity is currently finding numerous applications in the physical sciences [59, 60]. Finally, looking back at the opening sentence of this appendix, we perceive that we have come full circle, for the scientist is now learning what the man in the street has long known.

References

- [1] E. Fermi, J. Pasta, S. Ulam and M. Tsingou, Studies of nonlinear problems I, Los Alamos preprint LA-1940 (7 November 1955).
- [2] E. Fermi, Collected Papers, Vol. II (Univ. of Chicago Press, Chicago, 1965) p. 978.
- [3] H. Poincaré, Méthodes Nouvelles de la Mécanique Céleste, Vols. 1–3 (Dover Publ., New York, 1957), one may also consult a sometimes legible xerox translation: New Methods of Celestial Mechanics, Vols. 1–3 (NASA, Washington, DC, 1967).
- [4] G.D. Birkhoff, Dynamical Systems (Am. Math. Soc. Coll. Publ., New York (1927).
- [5] E. Fermi, Z. Phys. 24 (1923) 261.
- [6] D. ter Haar, Elements of Statistical Mechanics (Rinehart, New York, 1954).
- [7] W. Thirring, Classical Dynamical Systems (Springer, Berlin, 1978) p. 100.
- [8] J. Moser, Stable and Random Motions in Dynamical Systems (Princeton Univ. Press, Princeton, 1973) p. 41.
- [9] V.I. Arnol'd and A. Avez, Ergodic Problems of Classical Mechanics (Benjamin, New York, 1968).
- [10] V.I. Arnol'd, Russ. Math. Survey 18 (1963) N. 6, 85.
- [11] J.L. Tennyson, M.A. Liberman and A.J. Lichtenberg, AIP Conf. Proc. 57 (1979) 272.
- [12] B.V. Chirikov, J. Ford and F.V. Vivaldi, AIP Conf. Proc. 57 (1979) 323.
- [13] C.L. Siegel, Ann. Math. 42 (1941) 806;
J. Moser, Mem. Am. Math. Soc. 81 (1968) 1, discusses the significance of Siegel's theorem in a very readable review of stability in Hamiltonian systems.

- [14] E.T. Whittaker, *Analytic Dynamics* (Cambridge Univ. Press, Cambridge, 1965) Ch. 16.
- [15] A.N. Kolmogorov, in: *Lecture Notes in Physics* 93 (1979) 53.
- [16] J. Ford, *J. Math. Phys.* 2 (1961) 387.
- [17] J. Ford and J. Waters, *J. Math. Phys.* 4 (1963) 1293.
- [18] E.A. Jackson, *J. Math. Phys.* 4 (1963) 551, 686.
- [19] N.J. Zabusky and M.D. Kruskal, *Phys. Rev. Lett.* 15 (1965) 240;
N.J. Zabusky, in: *Nonlinear Partial Differential Equations* (Academic Press, New York, 1967) p. 223.
- [20] R.S. Northcote and R.B. Potts, *J. Math. Phys.* 5 (1964) 383.
- [21] P.C. Hemmer, L.C. Maximon and H. Wergeland, *Phys. Rev.* 111 (1953) 689.
- [22] G. Casati, J. Ford, F. Vivaldi and W.M. Visscher, *Phys. Rev. Lett.* 52 (1984) 1861.
- [23] J.L. Tuck and M.T. Menzel, *Adv. Math.* 9 (1972) 399.
- [24] M. Hénon and C. Heiles, *Astron. J.* 71 (1964) 393.
- [25] F.G. Gustavson, *Astron. J.* 71 (1966) 670.
- [26] M. Toda, *Phys. Rep.* 18 (1975) 1.
- [27] R. Abraham, *Foundations of Mechanics* (Benjamin, New York, 1967).
- [28] V.I. Arnol'd, *Russ. Math. Survey* 18 (1963) No. 5, 9.
- [29] J. Moser, *AIP Conf. Proc.* 57 (1979) 222.
- [30] G.D. Birkhoff, *Collected Mathematical Papers* (Am. Math. Soc., Providence, RI, 1950) Vol. I, p. 673; Vol. II, p. 252.
- [31] E. Zehnder, *Commun. Pure Appl. Math.* 25 (1973) 131.
- [32] J. Ford, in: *The New Physics* (Cambridge Univ. Press, Cambridge, 1989) p. 348.
- [33] F.M. Izrailev and B.V. Chirikov, *Sov. Phys. Dokl.* 11 (1966) No. 1, 30.
- [34] B.V. Chirikov, F.M. Izrailev and V.A. Tayursky, *Comput. Phys. Commun.* 5 (1973) 11.
- [35] B.V. Chirikov, *Phys. Rep.* 52 (1979) 263.
- [36] All the original papers describing these routes to chaos are reproduced in the anthology by: Hao Bai-Lin, *Chaos* (World Scientific, Singapore, 1984).
- [37] G.H. Walker and J. Ford, *Phys. Rev.* 188 (1969) 416.
- [38] J. Ford and G.H. Lunsford, *Phys. Rev. A* 1 (1970) 59.
- [39] E.T. Whittaker, *A Treatise on the Analytic Dynamics of Particles and Rigid Bodies* (Cambridge Univ. Press, Cambridge, 1965).
- [40] R.E. Peierls, in: *Theoretical Physics in the Twentieth Century*, eds. M. Fierz and V.F. Weisskopf (Wiley, New York, 1951).
- [41] M.W. Zemansky, *Heat and Thermodynamics* (McGraw-Hill, New York, 1951).
- [42] G. Casati, J. Ford, F.V. Vivaldi and W.M. Visscher, *Phys. Rev. Lett.* 52 (1984) 1861.
- [43] M.C. Wang and G.E. Uhlenbeck, *Rev. Mod. Phys.* 17 (1945) 323.
- [44] P. Martın-Löf, *J. Inf. Control* 9 (1966) 602.
- [45] G. Casati and J. Ford, *Phys. Rev. A* 12 (1975) 1702.
- [46] R.A. MacDonald and D.H. Tsai, *Phys. Rep.* 46 (1978) 1.
- [47] W.M. Visscher, in: *Methods in Computational Physics*, Vol. 15 (Academic Press, New York, 1976).
- [48] E.A. Jackson, *Rocky Mount. J. Math.* 8 (1978) 127.
- [49] F. Mokross and H. Büttner, *J. Phys. C* 16 (1983) 4539.
- [50] E.A. Jackson and A.D. Mistryotis, *J. Phys. Cond. Matter* 1 (1989) 1223.
- [51] P. Bocchieri, A. Scotti, B. Bearzi and A. Loinger, *Phys. Rev. A* 2 (1970) 2013;
P. Bocchieri and F. Valz-Gris, *Phys. Rev. A* 9 (1974) 1252;
G. Benetton, G. Lo Vecchio and A. Tennenbaum, *Phys. Rev. A* 22 (1980) 1709;
G. Benetton and L. Galgani, *J. Stat. Phys.* 27 (1982) 153;
R. Livi, M. Pettini, S. Ruffo, M. Sparpaglione and A. Vulpiani, *Phys. Rev. A* 31 (1985) 1039, 2740;
S. Isola, R. Livi, S. Ruffo and A. Vulpiani, *Phys. Rev. A* 33 (1986) 1163;
R. Livi, A. Politi, S. Ruffo and A. Vulpiani, *J. Stat. Phys.* 46 (1987) 147;
H. Kantz and P. Grassberger, *Phys. Lett. A* 123 (1987) 437;
H. Krantz, *Physica D* 39 (1989) 322.
- [52] A.J. Lichtenberg and M.A. Leiberman, *Regular and Stochastic Motion* (Springer, New York, 1983) p. 222.
- [53] Webster's Seventh New Collegiate Dictionary (G. & C. Merriam, Springfield, MA, 1963) p. 139.
- [54] Turing's statement and elegant proof of his halting theorem are reproduced in: G.J. Chaitin, *Adv. Appl. Math.* 8 (1987) 1.
- [55] G.J. Chaitin, *Information, Randomness, and Incompleteness* (World Scientific, Singapore, 1987).
- [56] B.V. Chirikov, F.M. Izrailev and D.L. Shepelyansky, *Physica D* 33 (1988) 77.
- [57] R.L. Devaney, *Chaotic Dynamical Systems* (Addison-Wesley, New York, 1989).
- [58] V.M. Alekseev and M.V. Yakobson, *Phys. Rep.* 75 (1981) 287 and references contained therein.
- [59] J. Ford, in: *Chaotic Dynamics and Fractals*, eds. M.F. Barnsley and S.G. Demko (Academic Press, New York, 1986).
- [60] W.H. Zurek, *Phys. Rev. D* 40 (1989) 1071; *Nature* 341 (1989) 119; *Phys. Rev. A* 40 (1989) 4731.